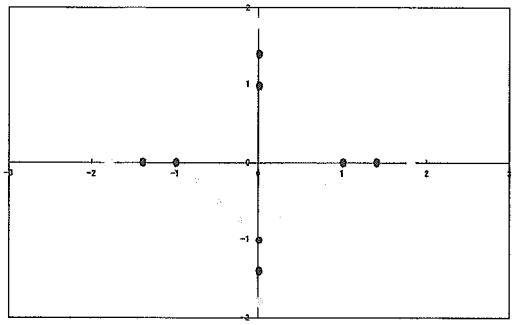

Figure 9: Average points.

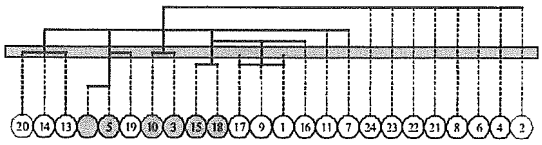

Figure 10: Hierarchical tree results from density-based clustering.

4.1.2 Results of Density-Based Clustering

We attempted to cluster with density-based clustering. In this two-dimensional test, we removed the normalization using the z-score. Figure 10 shows the results from using the density-based clustering algorithm with an imitative hierarchical tree.

Figure 11 is the 2 dimensional plot, which represents the clusters with the gray-labeled threshold in Figure 10. The black dots represent the core objects and the dotted ellipses show each cluster's core objects. The clusters in Figures 7 and 11 seem to be unrelated.

4.1.3 Result of MADIC

Figure 12 shows the results of our algorithm. This figure shows the hierarchical tree and appropriate clusters. Our algorithm found five clusters.

Figure 13 shows the classification results. The rigorous objects are black and an ellipse surrounds each cluster. Four of five clusters are the same as those seen in Figure 7. The fifth cluster, in the bottom right quadrant, contains object No. 18. This object has less deviation data than the producing rules. This finding illustrates that errors sometimes affect results. But, it appeared in the loosest threshold. We should use the results with the threshold that appeared. In gene expression analysis, we do analyze the clusters that appeared in the severe threshold.

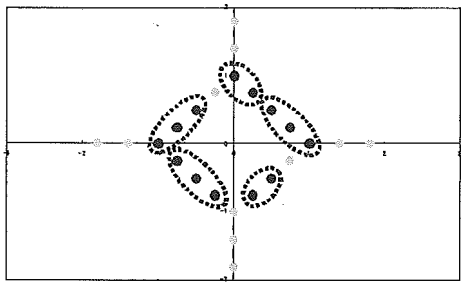

Figure 11: Results of density-based clustering.

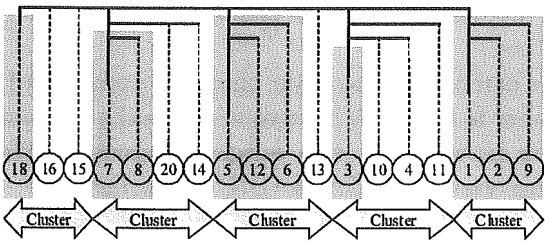

Figure 12: Results of our algorithm.

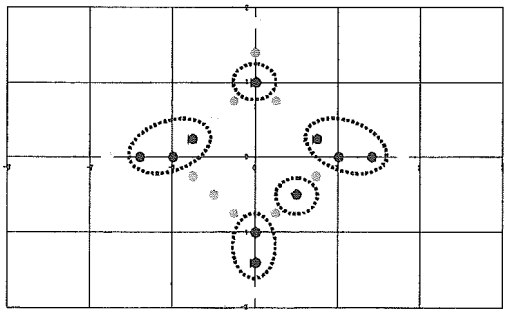

Figure 13: Classification results.

4.1.4 Comparison

Figure 14 shows the analysis flow. The generation rules exist but are always hidden; the objective of data mining is to discover these generation rules. If there are many observation points, we can discover the clusters, as seen in Figure 7. However, we sometimes obtain a limited number of observations.

We consider Figure 13 better than Figure 11. The proposed algorithm solves the new clustering problem. However, we cannot mathematically compare our algorithm and the existing algorithm.

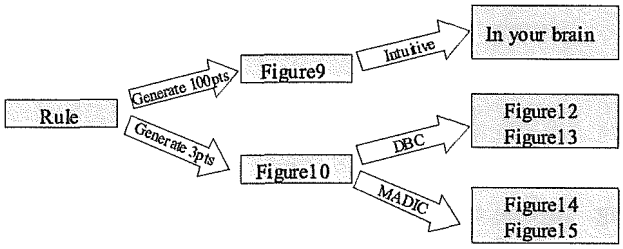

Figure 14: Analysis flow diagram.

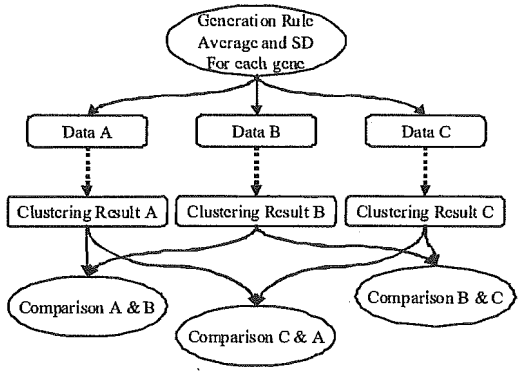

Figure 15: Synthetic data generation.

4.2 Experiment with 16-Dimensional Synthetic Data

4.2.1 Data

We used three data sets, each produced using the same rule. Each data set has 10,000 objects and 16 dimensions i.e. experimental conditions, and three data for each condition. Figure 15 shows the data generation, clustering, and comparison. We synthesized the average surfaces and then added to them random numbers. These data sets have the same characteristics, and therefore should generate the same clusters. However, the addition of random numbers generates the differences.

4.2.2 Evaluation Method

We added a big random number to simulate what we would see with real gene expression data. It is difficult to put them into the same cluster. We evaluated the number calculated by the following equation:

$$\text{Index} = \frac{\sum_{i,j=1}(\sharp(C_i C_j))^2}{\sqrt{\sum_{i=1}(\sharp(C_i))^2}\sqrt{\sum_{j=1}(\sharp(C_j))^2}}.$$

This equation shows the sum of squares of the number of intersections of both clusters, divided by the square roots of the sum of squares of the number of clusters.

This number is bounded from 0 to 1. If two clusters are completely the same, then this number is 1. If whole genes are grouped into one cluster, then this number is 1. So, we have to evaluate the number according to the number of clusters. We do the clustering experiments with various parameters. We gave the various numbers of clusters for k-means clustering various θ_m for MADIC clustering.

4.2.3 Results

We performed k-means clustering and MADIC clustering with various parameters (Figure 16). The indexes of the MADIC method are higher than those for k-means clustering. This result indicates that MADIC clustering is less affected by the random numbers than is k-means clustering.

4.3 Real Data

4.3.1 Data

NIHS performed experiments to determine how gene expression varied with exposure to four doses of thalidomide (vehicle only, low-dose, mid-dose, and high-dose) and four time points (2, 4, 8, and 24 hours later), i.e., 16 condition points with MOE430A of Affymetrix. Three mice were measured for each condition, creating triplicate data. Thus, 48 chips were used for the experiment.

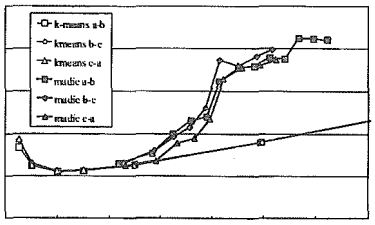

Figure 16: Results of 16-dimensional synthetic data.

Thalidomide is a drug for a sleeping aid and a treatment for morning sickness. It was subsequently found to be teratogenic, particularly during the first 25 to 50 days of pregnancy, most visibly causing amelia or phocomelia. The normalization was done by Percellome System for these measurement results. k-means clusterings were done for 16-dimensional data, averages for each condition with $k = 80$, 90, 100, compared with the MADIC result. It is difficult to predetermine the number of partitions, which is a very important parameter in k-means. AIC with EM method gave a partition number of one, which is obviously unacceptable; normally the number of clusters can only be determined from a biological viewpoint. In this study, partition numbers for k-means were the number of clusters given by MADIC.

4.3.2 Results

MADIC found 138 rigorous probes and 87 clusters. Moreover, 122 unique probes were found. These probes in clusters were summed up by the keywords in the Gene Ontology Biological Process. Ratios were calculated that had the same keywords in each cluster. Figure 17 shows the distributions of number of clusters for highest ratio of keywords in the Biological Process. MADIC could identify the clusters which have ratio more than 18%. This means that MADIC could find clusters which are assumed having biological meaning. Table 2 shows the average of the highest ratios of the same keyword. MADIC was higher than the k-means values. It is thought that this reflects division into the cluster that belongs to same key word in the Biological Process. The average about k-means was 10.514% and the standard deviation was 0.127%. The MADIC result was 6 SD from the k-means' average. This means that MADIC generated more homogenous clusters than k-means.

Table 2: Distribution of highest keyword.

k-means $N = 80$	10.369%
k-means $N = 90$	10.575%
k-means $N = 100$	10.599%
MADIC	11.445%

5 Conclusion

Traditional clustering algorithms cannot use all the data from repeated measurements. If deviations in repeated measurements are ignored, genes that have big errors can affect the results. Our experiment with 2-dimensional synthetic data shows better results than the k-means algorithm. Our experiment with 16-dimensional synthetic data shows the robustness to errors. In the experiment with real data, we assume MADIC creates the appropriate clusters.

The following features make MADIC a useful method for clustering results from gene expression experiments:

(1) MADIC can handle repeated measurements with error margins; it can identify more stable clusters for stable genes.

(2) The input parameters do not affect the clusters.

(3) Random seed numbers are not needed.

(4) Even if the number of members is one, a peculiar pattern can be extracted as a cluster.

By using our new algorithm, we were able to perform unsupervised clustering of all gene microarray data generated by the Percellome System. This algorithm provides a new option for the analysis of gene expression data.

Our algorithm adopts the gamma function as a density function. Even if an unstable object exists close to a stable object, as a characteristic of the gamma function the unstable object does not affect the stable object. However, because the gamma function does not permit integration by the odd number dimension, it cannot be applied to odd number dimension data. Moreover, it is believed that the device is necessary for very high dimensional data because the smoothness of the incomplete gamma function is lost.

Although our algorithm was designed to analyze microarray data, it should be useful for other types of data that retain error or variation information, and we will subsequently try to apply MADIC to other fields.

Acknowledgments

This work was supported by the Health Sciences Research Grant from the Ministry of Health, Labor and Welfare, Japan, H13-Seikatsu-012, H13-Seikatsu-013, H14-Toxico-001, and H15-Kagaku-002, and in collaboration with the NTT COMWARE CORPORATION.

References

[1] Ester, M., Kriegel, H. P., Sander, J., and Xu, X., A density-based algorithm for discovering clusters in large spatial databases with noise, *Proceedings of the Second International Conference on Knowledge Discovery and Data Mining*, 226–231, 1996.

[2] Kanno, J., Aisaki, K., Igarashi, K., *et al.*, "Per cell" normalization method for mRNA measurement by quantitative PCR and microarrays, (in preparation).

[3] Kumar, M., Patel, N. R., and Woo, J., Clustering seasonality patterns in the presence of errors, *Proceedings of the eighth ACM SIGKDD international conference Knowledge Discovery and data mining*, 557–563, 2002.

[4] Monti, S., Tamayo, P., Mesirov, J., and Golub, T., Consensus clustering: A resampling-based method for class discovery and visualization of gene expression microarray data, *Machine Learning*, 52:91–118, 2003.

[5] Papadopoulos, D., Domeniconi, C., Gunopulos, D., and Ma S., Clustering gene expression data in SQL using locally adaptive metrics, *Proceedings of the 8th ACM SIGMOD workshop on Research issues in data mining and knowledge discovery (DMKD 2003)*, 235–41, 2003.

[6] Yeung, K. Y., Medvedovic, M., and Bumbgarner, R. E., Clustering gene-expression data with repeated measurements, *Genome Biol.*, 4(5):R34, 2003.

Development 133, 1625-1634 (2006) doi:10.1242/dev.02344

Activation of Notch1 signaling in cardiogenic mesoderm induces abnormal heart morphogenesis in mouse

Yusuke Watanabe[1,*,†], Hiroki Kokubo[1,2,*], Sachiko Miyagawa-Tomita[3], Maho Endo[1], Katsuhide Igarashi[4], Ken ichi Aisaki[4], Jun Kanno[4] and Yumiko Saga[1,2,‡]

Notch signaling is implicated in many developmental processes. In our current study, we have employed a transgenic strategy to investigate the role of Notch signaling during cardiac development in the mouse. Cre recombinase-mediated Notch1 (NICD1) activation in the mesodermal cell lineage leads to abnormal heart morphogenesis, which is characterized by deformities of the ventricles and atrioventricular (AV) canal. The major defects observed include impaired ventricular myocardial differentiation, the ectopic appearance of cell masses in the AV cushion, the right-shifted interventricular septum (IVS) and impaired myocardium of the AV canal. However, the fates of the endocardium and myocardium were not disrupted in NICD1-activated hearts. One of the Notch target genes, *Hesr1*, was found to be strongly induced in both the ventricle and the AV canal of NICD1-activated hearts. However, a knockout of the *Hesr1* gene from NICD-activated hearts rescues only the abnormality of the AV myocardium. We searched for additional possible targets of NICD1 activation by GeneChip analysis and found that *Wnt2*, *Bmp6*, jagged 1 and *Tnni2* are strongly upregulated in NICD1-activated hearts, and that the activation of these genes was also observed in the absence of Hesr1. Our present study thus indicates that the Notch1 signaling pathway plays a suppressive role both in AV myocardial differentiation and the maturation of the ventricular myocardium.

KEY WORDS: Notch signaling, Heart formation, AV cushion, EMT

INTRODUCTION

The heart is the first functional organ to be formed during mouse development. Cardiac development is a complex process that requires myogenesis and morphogenesis to occur simultaneously with contractility. In addition, distinct cell populations have to be integrated in a temporally and spatially precise fashion. Cardiac mesoderm is specified in the anterior lateral mesoderm, which is a primary heart field, and then converges to form a linear heart tube along the ventral midline of the embryo. The heart tube grows rapidly in length through the addition of cells from the second heart field (Buckingham et al., 2005), and balloons to develop its atrial and ventricular compartments during looping. At the end of loop formation, the atria and ventricles are aligned and connected with each chamber through the atrioventricular (AV) canal. It has been suggested that the formation of this connection might involve rightward expansion of the AV canal (de la Cruz and Miller, 1968), leftward remodeling of the primary ventricular septum (Wenink, 1981) or reorganization of the AV myocardium (Kim et al., 2001a). The AV canal forms the AV cushions that are the primordia of the valves and membranous septae. They first become evident as localized swellings in the cardiac jelly, which are subsequently invaded by endothelial cells. The properties of both the AV endocardium and AV myocardium are distinctive in the AV canal. Recently, Notch signaling has been implicated in many aspects of heart development.

Notch is a transmembrane receptor and consists of several functional domains, a series of EGF and Notch/Lin12 repeats in the extracellular region, a transmembrane domain, a RAM domain, CDC10/ankyrin repeats and a PEST domain in the intracellular region (Reaume et al., 1992). Binding of Notch ligands, including delta-like (Dll) and jagged (Jag) proteins in mammals, to the corresponding Notch receptors leads to the stepwise cleavage of the receptor by specific proteases. As a result of this processing, the Notch intracellular domain (NICD) is released and transferred to the nucleus. The NICD then interacts with RBPjκ [also known as Su(H), CBF-1 and Lag-1; Rbpsuh – Mouse Genome Informatics], and regulates the transcription of the bHLH genes hairy/enhancer of split (*Hes*) and its related protein *Hesr* (also known as Hey, HRT, CHF, HERP), which then function as transcriptional suppressors of downstream targets (Artavanis-Tsakonas et al., 1999; Iso et al., 2003). In the mouse, *Notch1* begins to be expressed in the notochord and mesodermal tissues, including the posterior mesoderm, splanchnic mesoderm and extra-embryonic mesoderm at the primitive streak stage, and the *Notch1* expression profile in the heart is restricted to the endocardium by E8.0 (Williams et al., 1995). *Notch4* and one of its ligands, *Dll4*, are also expressed in the endocardium (Shirayoshi et al., 1997; Timmerman et al., 2004). *Notch2* expression in the heart cannot be detected by in situ hybridization during the early stages of development (Hamada et al., 1999), but the Notch2 protein is present in the atrial and ventricular myocardium at E13.5 (McCright et al., 2002). Although *Notch3* is expressed in the cardiogenic plate at the early headfold stage, it is no longer expressed at E8.0 (Williams et al., 1995).

Among the aforementioned Notch expression patterns, the restricted *Notch1* and *Notch4* expression in the endocardium during early heart development indicates that there is a crucial

[1]Division of Mammalian Development, National Institute of Genetics, Yata 1111, Mishima 411-8540, Japan. [2]Department of Genetics, The Graduate University for Advanced studies, Yata 1111, Mishima 411-8540, Japan. [3]Department of Pediatric Cardiology, The Heart Institute of Japan, Tokyo Women's Medical University, 8-1 Kawada-cho, Shinjyuku-ku Tokyo162-8666, Japan. [4]Cellular and Molecular Toxicology Division, National Institute of Health Sciences, 1-18-1 Kamiyohga, Setagaya-ku Tokyo 158-8501, Japan.

*These authors equally contributed to this work
†Present address: Department of Developmental Biology, Institute Pasteur, 25 rue du Dr Roux, 75015 Paris, France
‡Author for correspondence (e-mail: ysaga@lab.nig.ac.jp)

Accepted 23 February 2006

role for Notch signaling in endocardial development. Moreover, both *Notch1* and *Rbpsuh*-null mice have revealed in a previous study that Notch1/Rbpsuh signaling is essential for endocardial development and for EMT in the AV cushions (Timmerman et al., 2004). Recently, studies in human have shown that *Notch1* mutations cause defects in aortic valve formation (Garg et al., 2005). Moreover, the possible downstream target genes of Notch signaling, *Hesr1* and *Hesr2*, are crucial factors during cardiac development. These downstream genes show a complementary expression pattern in the heart: *Hesr1* is expressed in the atrium, outflow tract (OFT) and endocardium, and *Hesr2* is expressed in the ventricle (Leimeister et al., 1999; Nakagawa et al., 1999). *Hesr2*-null mice show defects in AV valve formation, and atrial and ventricular septal formation in the heart (Donovan et al., 2002; Gessler et al., 2002; Kokubo et al., 2004; Sakata et al., 2002). Intriguingly, *Hesr1/Hesr2* double knockout mice show a severe phenotype of impaired trabeculation, EMT and septation of the heart (Kokubo et al., 2005), although *Hesr1*-null mice do not show any detectable defects (Fischer et al., 2004; Kokubo et al., 2005).

The suppressive roles of Notch signaling have been reported during myocardial development in a number of different species. In *Xenopus* embryos, Notch signaling suppresses the expression of myocardial genes, as a result of which the heart precursor cells do not contribute to the myocardium (Rones et al., 2000). Similarly, in the *Drosophila* heart it has been shown that Notch activity, which is mediated by Su(H), prevents myocardial cell fate determination (Han and Bodmer, 2003; Park et al., 1998). Consistent with this finding, *Rbpsuh*-null ES cells show increased cardiomyogenic differentiation, which is likely to be due to the lack of Notch signaling (Schroeder et al., 2003). However, it is not yet clear whether Notch1 activity is involved in the determination of the cardiac fate in the mouse, as it is in both *Xenopus* and *Drosophila*.

A knockout strategy is both a straightforward and powerful method for elucidating gene function but transgenic strategies that use ectopic expression also yield valuable information. To elucidate the significance of the restricted Notch signaling in the endocardium, we investigated the effects of the forced expression of Notch1 in the myocardium, where the Notch signals are normally inactive. We speculated that this may provide an insight into the predominant expression of Notch1 in the endocardial cell lineage. For this purpose, we introduced NICD1 into the cardiac lineage of the mouse using the *Cre-loxP* system in *Mesp1-Cre* mice (in which a *Cre* recombinase gene is knocked into the *Mesp1* locus). Mesp1 is a bHLH transcription factor that is initially expressed in the invaginating mesoderm at the onset of gastrulation. Lineage analysis using *Mesp1-Cre* revealed that *Mesp1*-expressing cells mainly contribute to the endocardium and myocardium of the heart and to the endothelial cells of the embryonic and extra-embryonic blood vessels (Saga et al., 2000; Saga et al., 1999). The exception is observed in mesenchymal cells in the OFT derived from neural crest cells and some of the cells in the peripheral cardiac conduction system (Kitajima et al., 2006). In our present study, the expression of NICD1 in the entire cardiac lineage of the mouse has allowed us to determine the outcome of the forced expression of Notch1 in the myocardium lineage. The fates of the endocardium and myocardium were found not to be disrupted in NICD1-activated hearts but the forced activation of Notch signaling in myocardium results in the suppression of both the AV myocardial differentiation and the maturation of the ventricular myocardium.

MATERIALS AND METHODS

Generation of transgenic mice

The CAG-CAT-*NICD1* construct was generated by substituting *NICD1* (Takahashi et al., 2000) for β-galactosidase in the CAG-CAT-Z vector (Yamauchi et al., 1999). This construct was injected into fertilized eggs and permanent transgenic lines were established. The generation of *Mesp1-Cre* mice and *Hesr1*-null mice has been described previously (Kokubo et al., 2005; Saga et al., 1999). NICD1-activation of the cardiac lineage in mice was achieved by crossing CAG-CAT-*NICD1* mice with *Mesp1-Cre* mice. A TOPGal transgenic mouse line was established by injection of a vector containing *E. coli* β-galactosidase with the TOPflash promoter-enhancer (Upstate).

Histological analyses

For histological observations, Hematoxylin and Eosin staining was conducted on paraffin sections and ultrastructures were then observed by transmission electron microscopy (Miyagawa-Tomita et al., 1996). In situ hybridization analyses were performed using cRNA probes for *Notch1*, *Jag1*, *Bmp6*, *Hesr1*, *Hesr2*, troponin 1 fast-twitch skeletal muscle isoform (*Tnni2*), *Wnt2*, *Anf*, chisel (*Smpx* – Mouse Genome Informatics), *Bmp2*, *Tbx2*, *Cited1*, *Hand1* and *Bmp10*. The InsituPro system (M&S Instruments) was used for whole-mount in situ hybridizations according to the manufacture's instructions. Section in situ hybridizations were performed using 20 μm frozen sections. Activated-Notch1 was detected using an anti-cleaved Notch1 antibody (Val1744) (#2421, Cell Signaling Technology) with 6 μm paraffin sections. Other immunohistochemical detections were performed using anti-Myosin (Skeletal, Slow) (#M8421, Sigma) which is highly specific for the slow myosin heavy chain (Mhc), anti-α Smooth Muscle Actin (αSma) (#A2547, Sigma) and anti-CD31 (Pecam-1) (#557355, BD Biosciences) antibodies with 8 μm frozen sections.

RT-PCR analysis

Total RNA was isolated from the atria and ventricles of E10.5 mouse hearts using an RNeasy mini kit (Qiagen). cDNA was generated using SuperScript II reverse transcriptase (Invitrogen). PCR was performed using primers for *Hesr1* (5′-ACGACATCGTCCCAGGTTTTG-3′ and 5′-GGTGATCCAC-AGTCATCTGCAAG-3′), *Hesr2* (5′-GCTACAAGCTCAGTGATGAGG-3′ and 5′-GCCTGGAGCATCTTCAAATGATCC-3′), *Hes1*, *Hes5* (Kaneta et al., 2000), *Tnni2* (5′-CCAGCACTGCTGCACAGCA-3′ and 5′-AGACATGGAGCCTGGGATG-3′), *Wnt2* (Monkley et al., 1996), *Bmp6* (5′-AGCAACTAGCAATCTGTGGG-3′ and 5′-CGTTGTAGTCTGAA-GAACCG-3′) and *Jag1* (Timmerman et al., 2004). The number of PCR cycles was optimized for each reaction.

GeneChip analysis

Ventricles with an AV canal were isolated at developmental stage E10.5 and stabilized in RNA*later* RNA Stabilization Reagent (Ambion), prior to total RNA preparation. Total RNA isolates were purified using the RNeasy mini kit (Qiagen), according to the manufacturer's instructions. First-strand cDNAs were synthesized by incubating 5 μg of total RNA with 200 U SuperScript II reverse transcriptase (Invitrogen) and 100 pmol T7-$(dT)_{24}$ primer [5′-GGCCAGTGAATTGTAATACGACTCACTATAGGGAGG-CGG-$(dT)_{24}$-3′]. After second-strand synthesis, the double-stranded cDNAs were purified using a GeneChip Sample Cleanup Module (Affymetrix), according to the manufacturer's instructions. Labeling of the double-stranded cDNAs was achieved by in vitro transcription using a BioArray HighYield RNA transcript labeling kit (Enzo Diagnostics, Farmingdale, NY). The labeled cRNA was then purified using a GeneChip Sample Cleanup Module (Affymetrix) and treated with 1× fragmentation buffer (40 mM acetate, 100 mM KOAc, 30 mM MgOAc) at 94°C for 35 minutes. For hybridization to a GeneChip Mouse Genome 430 2.0 Array (Affymetrix), 15 μg of fragmented cRNA probe was incubated with 50 pM control oligonucleotide B2, 1× eukaryotic hybridization control (1.5 pM BioB, 5 pM BioC, 25 pM BioD and 100 pM Cre), 0.1 mg/ml herring sperm DNA, 0.5 mg/ml acetylated BSA and 1× manufacturer-recommended hybridization buffer in a 45°C rotisserie oven for 16 hours. Washing and staining were performed with GeneChip Fluidic Station (Affymetrix) using the appropriate antibody amplification, washing and staining protocol. The phycoerythrin-stained arrays were scanned as digital image files and scanned

data were analyzed with GeneChip Operating Software (Affymetrix). The GeneChip analyses were performed using two different RNA samples prepared from the control and NICD1-activated hearts, respectively. All data are available online (http://www.nihs.go.jp/tox/TtgSubmitted.htm) in the National Institute of Health Sciences.

RESULTS

Notch1 signal activation in the cardiac cell lineage of the mouse induces heart abnormalities

To investigate the possible role of Notch1 signaling during cardiac development in the mouse, we generated a transgenic line expressing *NICD1* cDNA, which comes under the control of the CAG promoter after excision of the floxed CAT gene by Cre recombinase (designated as CAG-CAT-*NICD1* mice). We used *Mesp1-Cre* mice to induce NICD expression in the cardiac cell lineage in transgenic progeny. By crossing with *Mesp1-Cre* mice, Cre/lox specific CAT excision occurs in *Mesp1*-expressing cells and results in the induction of *NICD1*-expression in the cardiac lineages (designated as NICD1-activated mice). Whole-mount in situ hybridization experiments subsequently revealed a appreciable level of *Notch1* induction in the hearts of NICD1-activated mice (NICD1-activated hearts), which exhibited a deformed shape with a rough surface morphology (Fig. 1C,D). The transgenic mice did not develop beyond embryonic day 10.5 (E10.5) and died before E11.5. These heart abnormalities are clearly distinguishable from wild-type mice (Fig. 1A,B).

To confirm Notch1 activation, we performed immunohistochemical staining using antibodies against processed-NICD1. In wild-type hearts, Notch1 activation was observed only in the endocardium (Fig. 1E-H), but neither in myocardium or mesenchymal cells derived from the endocardium of the AV canal. By contrast, activated Notch1 was observed in the entire heart, including the endocardium, the myocardium of both the atria and ventricles, and the AV cushions, in NICD1-activated embryos (Fig. 1I-L). We were therefore able to conclude that Notch activation was successfully induced in the entire cardiac lineage in our double transgenic mice.

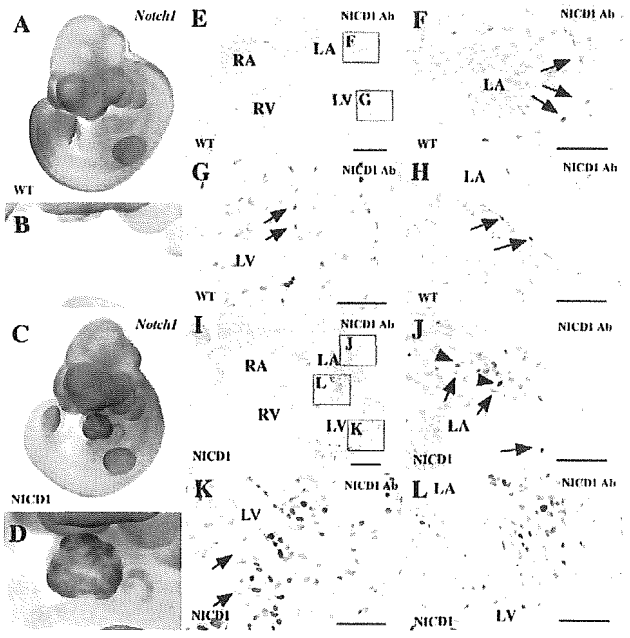

Fig. 1. Notch activation in the mouse cardiac cell lineage.
(A-D) *Notch1* expression revealed by whole-mount in situ hybridization at E10.5. In wild-type embryos (A,B), it is difficult to detect Notch1 expression in the heart at the whole-mount level, whereas in NICD1-activated hearts (C,D), *Notch1* is strongly induced in whole heart which shows an abnormal morphology. The heart regions are magnified (B,D). **(E-L)** Immunohistochemical analysis of cleaved-Notch1 (NICD1 Ab) at E10.5. NICD1 signals are only observed in the nuclei of endocardial cells in the wild-type heart (E-H), whereas the signals are observed in both endocardial and myocardial cells in NICD1-activated hearts (I-L). The images of other sections were generated to indicate that only endocardial cells are NICD1-positive in the AV cushion of the wild-type embryonic heart (H). Arrows indicate endocardial cells. Arrowheads indicate myocardial cells. Abbreviations: LA, left atrium; RA, right atrium; LV, left ventricle; RV, right ventricle. Scale bars: 200 μm in E,I; 50 μm in F-H,J-L.

Myocardial defects in the NICD1-activated heart

Histological observations by H&E staining, followed by marker analyses, revealed four major defects in NICD1-activated hearts: (1) impaired ventricular myocardial differentiation; (2) the ectopic appearance of cell masses in the AV cushion; (3) right-shifted IVS; and (4) impaired myocardium of the AV canal. Aberrant myocardial trabeculation was the first anomaly to be observed (Fig. 2A,B). In the wild-type mouse heart, the trabeculae extend to the inner space of the ventricle from the compact layer that has a thickness of two to three cells (Fig. 2A). By contrast, the trabeculae were found to have accumulated in the ventricular wall in NICD1-activated hearts (Fig. 2B). The abnormal accumulation of trabecular cells near the compact layer is likely to be the cause of the rough external appearance of the ventricle (Fig. 1D). To investigate possible alterations in the properties of the trabecular cells in the NICD1-activated heart, we examined the expression of *Bmp10*, which is a gene that is known to be specifically expressed in the trabecular cells and to be important for the growth of trabecular myocardium (Fig. 2C) (Neuhaus et al., 1999). *Bmp10* expression was detected in the NICD1-activated heart, indicating that the trabecular cells were not strongly affected by Notch1 activation (Fig. 2D). However, this expression was not detected in the trabeculae of the AV myocardium (asterisk in Fig. 2D) (see below).

To examine the possibility that Notch1 signaling influences the fate decisions of the myocardium in mouse, as is the case in *Drosophila* and *Xenopus* (Han and Bodmer, 2003; Rones et al., 2000), we analyzed the expression of cell-type specific markers by RT-PCR and immunohistochemical staining. Semi-quantitative RT-PCR analysis showed no detectable changes in the expression of the myocardial genes, myosin light chain (*Mlc*) 2a (*Myl7* – Mouse Genome Informatics), *Mlc2v* (*Myl2* – Mouse Genome Informatics), *Mhca* (*Myh6* – Mouse Genome Informatics), *Nkx2.5*, *Mef2c* and *Gata4* in the ventricle (see Fig. S1 in the supplementary material). Although *Mhcb* (*Myh7* – Mouse Genome Informatics) appears to be induced in the atrium of NICD1-activated hearts, this might be due to contamination of the expanded left ventricle. We also examined protein markers such as Mhc, αSma (for myocardium) and Pecam (for endocardium) using specific antibodies. Although we found no significant changes in the expression patterns of Mhc and αSma, except for the AV canal (Fig. 2F, H, see below), Pecam expression was significantly reduced in the endocardium surrounding the trabecular cells in NICD1-activated hearts (Fig. 2J). Furthermore, Pecam-positive cells were often observed in the interventricular septum (IVS, see arrowheads in Fig. S2 in the supplementary material),which may indicate anomalies in the myocardium of the IVS. To further investigate these transgenic embryos for possible defects in the trabecular cells, we examined their fine structures by

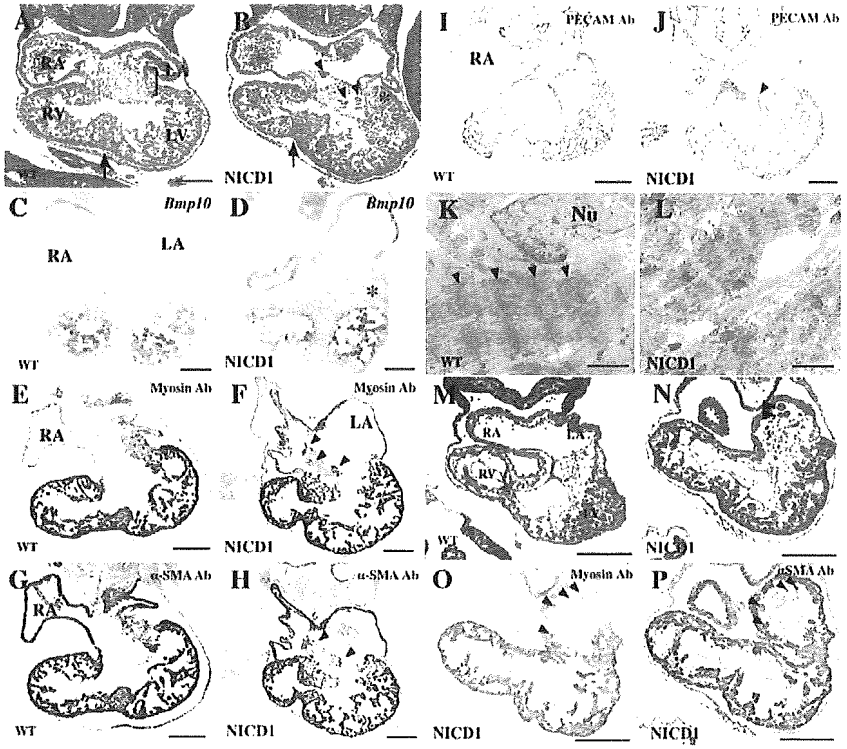

Fig. 2. Morphological and histological defects induced by NICD1-activation. (**A,B**) Sections stained with Hematoxylin and Eosin show normal EMT in the AV cushion (brackets) and trabecular development in wild-type hearts (A), whereas the trabeculae are not formed normally in NICD1-activated hearts (B). Ectopic cell masses were also evident (arrowheads in B), the interventricular septum is right-shifted (arrow) and trabeculation occurs in the AV myocardium (asterisk in B) in NICD1-activated hearts. (**C,D**) *Bmp10* expression was observed in the trabecular cells in both the wild-type (C) and NICD1-activated (D) ventricles. (**E-J,O,P**) Immunohistochemistry using anti-myosin (E,F,O), anti-α-smooth muscle actin (αSma) (G,H,P) and anti-Pecam (I,J) antibodies reveal that ectopic cell masses (arrowheads) are present in the cushion tissue in NICD1-activated hearts (F,H,J,O,P), but are never observed in wild-type hearts (E,G,I). (**M,N**) Hematoxylin and Eosin staining at E9.5 also shows ectopic cell masses in the cushion of NICD1-activated heart (arrowheads in N) but not in wild-type heart (M). (**K,L**) In wild-type myocardium (K), myofibrils with sarcomere structures (Z bands are indicated by black arrowheads) are observed by transmission electron microscopy, but only thin myofibrils without a proper sarcomere structure (no Z band indicated by while arrowheads) are formed in NICD1-activated hearts (L). Embryo samples were prepared at either E10.5 (A-L) or E9.5 (M-P). Serial sections were used for E,G,I (wild-type), F,H,J (NICD1-activated) and N-P (NICD1-activated). Abbreviations: LA, left atrium; RA, right atrium; LV, left ventricle; RA, right ventricle; Nu, nucleus. Scale bars: 200 μm in A-J,M-P; 1 μm in K,L.

transmission electron microscopy. At this stage, myofibrils are found to be well developed in the wild-type mouse heart and the sarcomere structures with Z bands were well organized in the wild-type trabecular myocardial cells (Fig. 2K). In NICD1-activated hearts, however, the myofibrils were poorly formed with an unclear sarcomere structure (Fig. 2L), indicating that myocardial maturation is inhibited in NICD1-activated hearts. These results indicate that Notch1 signaling does not influence the fate of myocardial cells in the mouse, but it acts as an inhibitor of myocardial differentiation, which is associated with abnormal trabeculation in the ventricle.

Appearance of ectopic cell masses in the AV cushion in the NICD1-activated heart

The second principal anomaly of the NICD1-activated heart that we observed occurs in the AV cushion. For the formation of the AV cushion, a subset of endocardial cells that overlie the AV canal undergoes endothelial-mesenchymal transformation (EMT), followed by invasion of the cardiac jelly. In NICD1-activated hearts, mesenchymal cells in the AV cushion were found, indicating that EMT events seemed to occur normally. However, ectopic cell masses were detected in the cushion tissue (Fig. 2B, arrowheads). Immunohistochemical analyses identified that these cell masses were Mhc- and αSma-positive (arrowheads in Fig. 2F,H), but Pecam negative (arrowhead in Fig. 2J), suggesting that these cells possess myocardial properties. It is noteworthy that these cells were never observed in wild-type cushion tissues at E10.5 (Fig. 2E,G). To determine how such ectopic cells develop in the NICD1-activated heart, we observed then at E9.5, when it is known that EMT starts to occur in the AV cushion. As is clearly shown in Fig. 2N, we found ectopic cell masses, which were Mhc- and αSma-positive (Fig. 2O,P), in the NICD1-activated heart but not in the wild-type samples (Fig. 2M). Furthermore, serial Hematoxylin and Eosin staining of sections along the AP axis indicated that these cells were derived from the myocardial cells located at the AV canal, where trabeculation does not generally occur at this stage (see Fig. S3 in the supplementary material).

IVS shift and AV myocardial defect in the NICD1-activated heart

The third anomaly of the NICD1-activated mouse heart is the noticeable difference in the size of the ventricles. The left ventricle in the NICD1-activated mouse appears to be expanded, whereas the

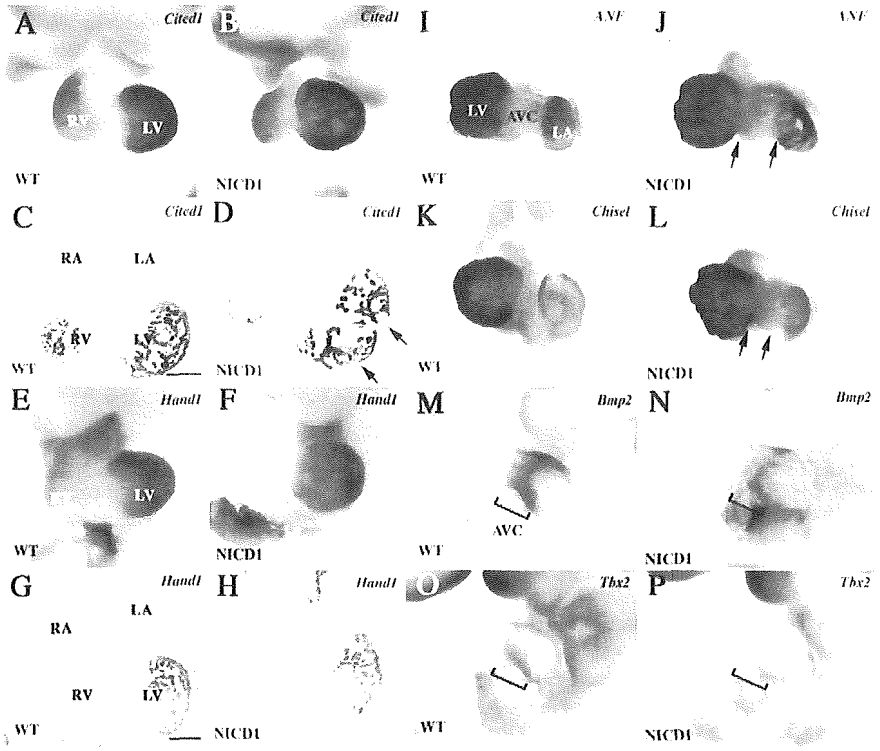

Fig. 3. Molecular characterization of defects in NICD1-activated hearts. The differences between the right and left ventricles were examined by whole mount (A,B,E,F) or section (C,D,G,H) in situ hybridization using probes *Cited1* (**A-D**) or *Hand1* (**E-H**). To demarcate the boundaries between both the atrial and ventricular chambers and the AV canal, chamber markers *Anf* (**I,J**), *Smpx* (**K,L**) and AV canal markers *Bmp2* (**M,N**) and *Tbx2* (**O,P**) were used as probes. Boundaries between the chambers and AV canal became less evident in the NICD1-activated heart (indicated by arrows in J and L). AV canal marker expression is also downregulated in the NICD1-activated hearts (indicated by brackets in M-P). Abbreviations: LA, left atrium; RA, right atrium; LV, left ventricle; RA, right ventricle. Scale bars: 200 μm in C,G.

right ventricle is reduced in size, compared with wild type. In addition, the position of the IVS that separates the right and left ventricles is shifted to the right side in the NICD1-activated mouse (compare arrows in Fig. 2A with 2B). However, no enhanced cell proliferation was observed in the left ventricles of NICD-activated hearts (data not shown), indicating that the property of each ventricle might be affected by Notch1 activation. The expression of *Cited1*, which is negative in the IVS, revealed differences in size between the right and left ventricles (Fig. 3A-D). We found cells showing reduced *Cited1* expression in the NICD1-activated heart (arrows in Fig. 3D), which may indicate abnormalities in cardiomyocyte differentiation. Furthermore, the expression of *Hand1*, which is a known marker for the left ventricle (Fig. 3E,G), showed expanded expression in the NICD1-activated heart (Fig. 3F,H).

It was also noted that the AV myocardial wall shows evidence of trabeculation in NICD1-activated mice (Fig. 2B,D,F,H,J,N,O,P; Fig. 3D,H). The properties of the chamber and AVC region were examined by molecular analyses using the chamber markers *Anf* and *Smpx* (*Chisel*) to demarcate the ventricles and atria (Fig. 3I-L), and *Bmp2* and *Tbx2* to characterize the AV canal (Fig. 3M-P). In the NICD1-activated heart, AVC marker expression, *Tbx2* in particular, is greatly reduced (Fig. 3P). In addition, the *Anf* and *Smpx* expression patterns revealed enlarged left ventricles and ambiguous AV boundaries (arrows in Fig. 3J,L). In the wild-type heart, the AV canal allows the endocardium to develop AV cushion tissue by EMT (Fig. 2A, brackets) and even though the AV myocardium shows weak Mhc and αSma staining in the wild-type heart (Fig. 2E,G), the trabeculae never develop in the AV myocardium at this stage. This indicates that the properties of the AV myocardium are distinct from the chamber myocardium. However, in the NICD1-activated heart, AV cushion tissues were formed and the trabeculae could be observed in the expected AV canal, which may indicate a lack of AV myocardial characteristics (Fig. 2B, asterisk).

Hesr1 is ectopically induced in the NICD1-activated ventricle

Hes and Hesr family members are known to be downstream targets of Notch signaling (Iso et al., 2003). We therefore examined whether these genes are induced in NICD1-activated hearts. RT-PCR and in situ hybridization analyses revealed that the expression of *Hesr1* and *Hesr2* is restricted to the myocardium of the atria and ventricles of wild-type hearts, respectively (Fig. 4A,B,D), which is consistent with previous reports (Leimeister et al., 1999; Nakagawa et al., 1999). However, in NICD1-activated hearts, *Hesr1* was found to be ectopically induced at high levels in the myocardium of the ventricle (Fig. 4A,C), whereas *Hesr2* was not shown to be induced in the myocardium of the atrium (Fig. 4A,E). Intriguingly, *Hesr1* was not expressed in the endocardium at this stage, despite the activation of Notch1 (Fig. 4B, Fig. 1G). A noticeable change was also observed in the AV myocardium of the transgenic hearts, in which the extended trabeculation appeared to be coincident with the co-expression of *Hesr1* and *Hesr2*. As *Hesr2* expression occurs in the wild-type ventricle, ectopic *Hesr1* expression might be the cause of the ventricle and AV canal defects in the NICD1-activated mice. In addition, *Hes5* expression was induced in both the atria and ventricles in Notch1-activated hearts (Fig. 4A), although it is not expressed in the wild-type heart.

NICD1 activation in a *Hesr1*-null background rescues the AV myocardium defect

Hesr1 is strongly induced in the NICD1-activated mouse heart and is known to be a transcriptional repressor, which lead us to hypothesize that the major cardiac defects observed in NICD1-activated mice might be caused by the ectopic expression of *Hesr1*. To examine this possibility, we generated NICD1-activated mice in a *Hesr1*-null background. *Hesr1* knockout mice show no detectable defects in heart morphogenesis (Fig. 5A,C,E) (Kokubo et al., 2005).

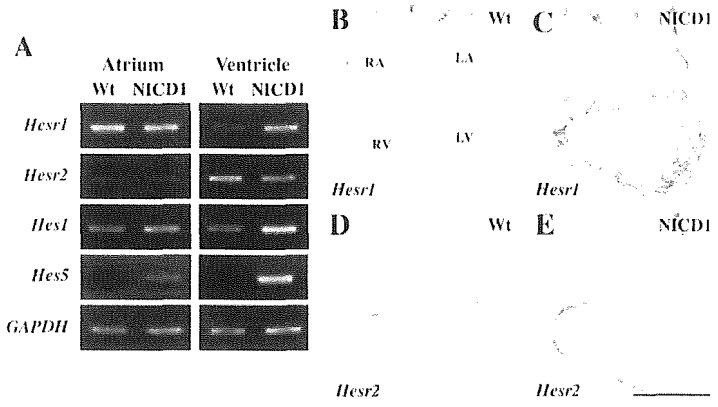

Fig. 4. Expression changes in the *Hes* and *Hesr* gene families at E10.5. (**A**) Semi-quantitative RT-PCR analysis showing upregulation of *Hesr1*, *Hes1* and *Hes5* in NICD1-activated hearts. *Hesr1* is ectopically induced at particularly high levels in the ventricle. In situ hybridization analysis also revealed the ectopic induction of *Hesr1* in the ventricle and AV canal of NICD1-activated hearts (**C**), whereas *Hesr1* is expressed only in the atrium in wild-type hearts (**B**). In contrast to *Hesr1*, *Hesr2* is expressed in the ventricle in wild-type hearts (**D**) and its distribution is not altered in NICD1-activated hearts (**E**). Abbreviations: LA, left atrium; RA, right atrium; LV, left ventricle; RA, right ventricle. Scale bar: 500 μm in E.

Hence, if the defects in NICD1-activated hearts were due to the suppression of specific genes by elevated *Hesr1*, we would expect that they would be rescued by the absence of Hesr1. Unexpectedly, however, most of defects observed in NICD1-activated hearts were also elicited by Notch1 activation, even in the absence of *Hesr1* (Fig. 5A-D, Fig. 1A-D). In the NICD1-activated/*Hesr1*-null hearts, impaired ventricular trabeculation and cell masses in the cushion tissue (Fig. 5F, arrowhead) were again observed, as seen in NICD1-activated hearts (Fig. 2B). However, we observed that there was much less trabeculation of the AV myocardium in the NICD1-activated/*Hesr1*-null background, suggesting that the property of the AV myocardium is recovered (Fig. 5F, brackets), whereas the IVS was again right-shifted (Fig. 5F, arrow). These data indicate that ectopic *Hesr1* expression in the myocardium may have caused the defects observed in the AV myocardium.

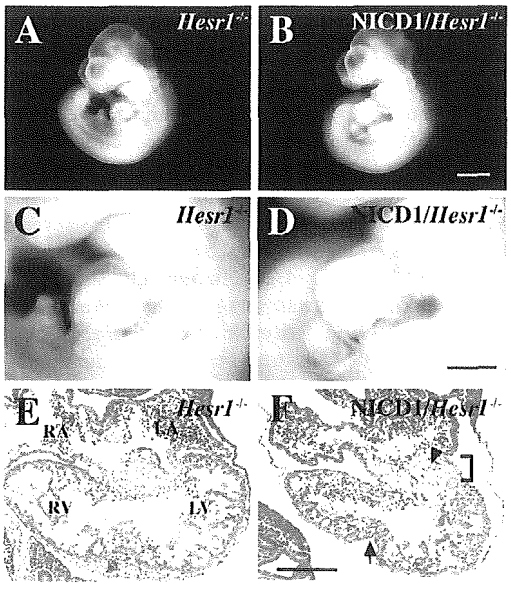

Fig. 5. NICD1-activated hearts in a *Hesr1*-null background at E10.5. *Hesr1*-null mice do not show any detectable defects (**A**,**C**,**E**) and NICD1-activation in *Hesr1*-null induced heart defects (**B**,**D**) is similar to NICD-activation in Hesr1-positive mice. Hematoxylin and Eosin analysis also revealed impaired trabeculation, the appearance of cell masses in the AV cushion (arrowhead) and a right-shifted interventricular septum (arrow). However, the AV myocardium is recovered (brackets) (**F**). Abbreviations: LA, left atrium; RA, right atrium; LV, left ventricle; RA, right ventricle. Scale bar: 1 mm in B; 500 μm in D; 200 μm in F.

Wnt2, *Bmp6*, *Tnni2* and *Jag1* are induced in NICD1-activated hearts

As it was unlikely that Hesr1 would be the sole mediator of Notch1 signaling, and because Hesr1-independent mechanisms must be involved in the formation of the defects in NICD1-activated hearts, we examined the expression of several genes that could potentially be involved in these myocardial abnormalities. However, following RT-PCR experiments, we could not find any critical changes in the expression levels of the genes that we selected for analysis (*Mlc2a*, *Mlc2v*, *Mhca*, *Mhcb*, *Nkx2.5*, *Mef2c*, *Gata4*, *Nrg1*, *Erbb4*, *Ccnd1*, *Jmj*, *Snail*) (Supplementary Fig. S1). Therefore, to identify candidate genes that are differentially regulated in NICD1-activated hearts, we performed comparative GeneChip analysis using RNA isolates from ventricles with an AV canal from transgenic and wild-type hearts at E10.5. These experiments identified several genes showing differences in their expression levels between wild-type and NICD1-activated mice. Since we had observed that the lack of Hesr1, which is known to function as a transcriptional suppressor (Iso et al., 2001b), only rescues the AV myocardium, we focused on genes that were upregulated in NICD1-activated hearts (see Table S1 in the supplementary material). Among the candidates that we analyzed were *Wnt2*, *Bmp6* and troponin 1 fast-twitch skeletal muscle isoform (*Tnni2*), which we subsequently confirmed by RT-PCR and in situ hybridization (Fig. 6). In wild-type hearts, *Wnt2* is expressed strongly in the posterior region, e.g. the sinus venosus (Monkley et al., 1996) and the atrium, but it is difficult to detect its expression in the ventricle of wild-type hearts (Fig. 6B,B′). However, *Wnt2* expression was easily detectable in NICD1-activated hearts (Fig. 6C). Transverse sections also revealed stronger ectopic expression of *Wnt2* in the left ventricle, including the AV canal (Fig. 6C′).

Similar expression changes was observed for *Bmp6* (Fig. 6D-E′), which is normally expressed in the OFT and cushion tissue (Kim et al., 2001b). In wild-type hearts, *Tnni2* expression was found to be marginally expressed in the atrium (Fig. 6F,F′), but to be strongly induced both in the atria and the ventricles in NICD1-activated hearts (Fig. 6G,G′). Tnni2 is one of the components of troponin 1, and is known to inhibit the interaction between actin and myosin in the absence of Ca^{2+} (Clark et al., 2002; Gordon et al., 2000). Hence, the elevated expression of *Tnni2* might be one of the leading causes of the induction of the myocardial structural defects in NICD1-activated mice. We observed that one of the known Notch ligands,

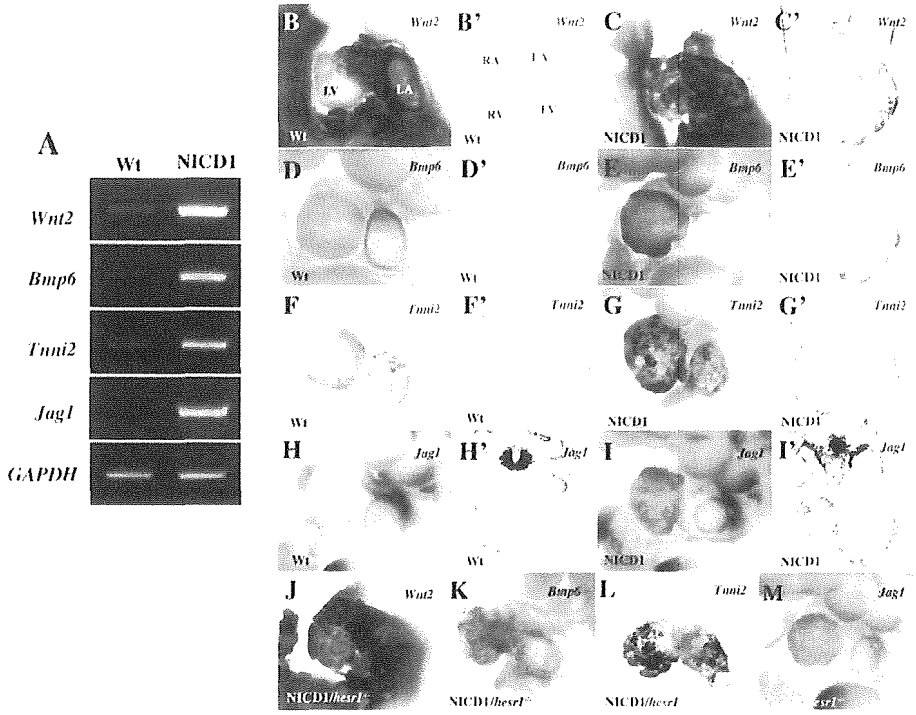

Fig. 6. Upregulation of *Wnt2*, *Bmp6*, *Tnni2* and *Jag1* in NICD1-activated hearts at E10.5. (**A**) RT-PCR analysis was performed using RNA from the ventricle with the AV canal. Expression of *Wnt2*, *Bmp6*, *Tnni2* and *Jag1* is upregulated in NICD1-activated hearts (**B-I'**) Whole-mount and section in situ hybridization confirmed the upregulation of these genes (B,B',D,D',F,F',H,H', wild-type hearts; C,C',E,E',G,G',I,I', NICD1-activated hearts). The upregulation is also observed in NICD1-activated hearts in a *Hesr1*-null background (**J-M**). Abbreviations: LA, left atrium; RA, right atrium; LV, left ventricle; RA, right ventricle.

Jag1, is also induced in NICD1-activated hearts (Fig. 6A). *Jag1* is expressed in the atria, right ventricle and OFT of wild-type hearts (Fig. 6H,H'), and this expression was found to be expanded into the whole heart in NICD1-activated mice (Fig. 6I,I'). We also examined the distribution of these genes at E8.5 to determine whether their expression profiles are affected from an earlier stage. Although the upregulation of NICD1 expression was not clear in the NICD1-activated hearts at this stage (see Fig. S4A,B in the supplementary material), we observed increased expression of the above genes and also morphological changes (rough surface) in NICD1-activated hearts (see Fig. S4D,F,H,J in the supplementary material).

As all of these expression changes coincide with the *Hesr1* expression pattern, we speculated that they are in fact the result of secondary effects of Hesr1 induction. To address this possibility, we examined the expression of each of these genes in the NICD1-activated hearts of Hesr1 knockout mice. As shown in Fig. 6J-M, elevated gene expression was observed for *Wnt2*, *Bmp6*, *Tnni2* and *Jag1*, even in the absence of Hesr1. These data indicate that the activation of these genes is either mediated by a factor other than Hesr1 or is directly regulated by NICD1.

DISCUSSION

In this study, we have generated NICD1-activated mice and analyzed their cardiac lineage. NICD1-activated hearts showed abnormal morphologies, such as disrupted cardiomyocyte differentiation, the appearance of ectopic cell masses in the AV cushion, a right-shifted IVS and defects in the AV myocardium. Moreover, these NICD1-activated mice died at E10.5. It has been shown that the AV myocardium is important for connection formation between the right atrium and right ventricle, and the left atrium and left ventricle at the end of looping (Kim et al., 2001a). Furthermore, it has been suggested that the AV node develops from that part of the AV canal myocardium. Therefore, we speculate that the transgenic embryo does not form a complete heart with normal cardiac morphology and conduction system, resulting in death at an early stage. Comparisons with NICD1-activated hearts in a *Hesr1*-null background demonstrate that ectopic *Hesr1* expression is responsible for the differentiation of the AV myocardium. In NICD1-activated hearts, the expression of *Wnt2*, *Bmp6*, *Tnni2* and *Jag1* could be induced in addition to *Hesr1*, and this might well be the cause of these myocardial abnormalities.

The involvement of Notch signaling in cardiac cell fates

In *Xenopus*, the expression of *Serrate1* (*Xenopus Jag1*) and *Notch1* overlaps in the dorsal side of the heart, and the forced expression of the activated form of Su(H) (*Xenopus* RBPjκ) suppresses the expression of myocardial genes (Rones et al., 2000). This indicates that Jag1-Notch1 signaling in *Xenopus* has an inhibitory effect upon myocardial fate determination. Although the expression levels of myocardial genes were shown previously not to change in either NICD1-activated, *Notch1* or *Rbpsuh* mutant hearts (Timmerman et al., 2004), our current histological data suggests that Notch1 signaling suppresses myocardial differentiation but does not affect myocardial cell fate decisions. In addition, the ectopic expression of Su(H) in *Xenopus* embryos results in the reduction of the number of myocardial cells that contribute to the heart (Rones et al., 2000). In the mouse, by contrast, abnormal trabeculation of the AV myocardium was observed in NICD1-activated hearts and this defect was rescued by a lack of Hesr1, which indicates that Notch/Hesr1 signaling might have suppressive effects for AV myocardial differentiation in the mouse.

The suppressive effects of Notch1 signaling on cardiomyocyte maturation

We observed the suppression of myocardial differentiation in NICD1-activated hearts and confirmed the presence of myofibrillar disorganization in their trabeculae by TEM analyses. Notch1

signaling in the wild-type mouse heart is restricted to the endocardial cells, as we observe Notch1 activation by antibody staining only in the endocardium. In NICD1-activated hearts, however, Notch1 signaling is also activated in the myocardium. Therefore, it is likely that the ectopic Notch1 activation in myocardium may directly suppresses differentiation, but it is also possible that secreted factor(s) from the endocardium (Bmp6 and Wnt2 are the candidates), that might be activated by additional NICD1, negatively regulate cardiomyocyte differentiation. If this is indeed the case, we speculate that Notch1 signaling negatively regulates cardiomyocyte differentiation. However, the effects of Notch1/Rbpsuh signaling upon myocardial development are not fully clear because heart formation itself is severely retarded in *Rbpsuh*-null mutants (Timmerman et al., 2004). We also have investigated conditional knockout embryos for the *Rbpsuh* allele driven by *Mesp1-Cre*. However, the resulting phenotype was similar to that of the *Rbpsuh*-null embryo and the heart was underdeveloped (data not shown), possibly owing to the early onset of *Mesp1*.

The role of Notch1 signaling in the AV myocardium

In our current experiments, Mhc, αSma-positive and Pecam-negative cell masses were observed in the AV cushion of NICD1-activated hearts. From our observations of serial sections of NICD1-activated hearts, we postulate that these cell masses could originate from the AV myocardium, where trabeculation is normally prevented in the wild-type AV canal. Bmp2 is a crucial factor in the determination of AV myocardial identity by regulating *Tbx2* and its downstream genes, including *Anf* and *Smpx* (Ma et al., 2005). In the NICD1-activated heart, the decreased expression of *Bmp2* and *Tbx2* in the AV myocardium should cause the loss of an AV identity, which in turn might confer the chamber identity to the AV canal, as evidenced by ambiguous *Anf* and *Smpx* expression. This may also induce ectopic trabeculation in the AV myocardium. The other possibility that we have considered for the origins of the cell masses are the endocardial cells. This is based upon the severe defects that can be observed in endocardial development and EMT in both *Notch1* and *Rbpsuh*-null mice (Timmerman et al., 2004). Furthermore, it has been reported that Notch1 activation induces the transformation of either AV canal explants or endothelial cells to αSma-positive cells (Noseda et al., 2004; Timmerman et al., 2004). Although it is not clear whether these transformed cells also express Mhc, the cell masses in the NICD1-activated AV cushion might well be derived from endocardial cells due to excess EMT.

Implications of the upregulated genes identified in NICD1-activated mouse hearts

In vitro experiments have indicated that both *Hesr1* and *Hesr2* are induced by NICD1 (Iso et al., 2002; Iso et al., 2001a; Nakagawa et al., 2000). However, in NICD1-activated hearts, *Hesr1* was strongly induced but not *Hesr2*, suggesting that the regulatory mechanism is different between these genes. A possible function for the Hes proteins in these events, as they are also induced in NICD1-activated hearts, will need to be addressed in future studies.

In addition to Hes family genes, we have found that many genes are induced in NICD1-activated hearts. Among these, the upregulation of *Tnni2* might be responsible for the observed myocardial defects. In the mouse heart, the most abundant troponin I is *Tnni3* (cardiac *Tnni*), but *Tnni2* is also transiently expressed in embryonic hearts from E9.5 to E16.5 (Zhu et al., 1995). *Tnni2* mutant mice have not been reported, but *Tnni3* mutant mice have been generated and show shortened sarcomere lengths (Huang et al., 1999). A single *Tnni* gene has been identified in *Drosophila*; its mutant, *hdp*^{3}, exhibits impaired sarcomere structure (Nongthomba et al., 2004). The strong induction of *Tnni2* by NICD1 may therefore be one of main causes of the disrupted sarcomere structure in NICD1-activated hearts. *Wnt2* is normally expressed in early cardiac mesoderm and thereafter in the sinus venosus and OFT regions (Monkley et al., 1996). However, signals detected using a LEF/TCF reporter (TOPGal) did not differ between wild-type and NICD1-activated hearts (see Fig. S5 in the supplementary material), which suggests that Wnt2 uses a non-canonical Wnt pathway in the mouse heart. Recently, it has been shown that a non-canonical Wnt11 signaling pathway is crucial for cardiogenesis and cardiomyocyte differentiation (Pandur et al., 2002; Terami et al., 2004), and that its expression pattern overlaps in the OFT with Wnt2. These non-canonical Wnt signaling mechanisms must therefore be involved in cardiogenesis.

We also demonstrate in our current experiments that there is a strong induction of *Bmp6* by Notch1 signaling. The importance of BMP6 signaling during cardiac development was previously reported by the analysis of *Bmp6/Bmp7* double-null mice, which showed retarded OFT cushion development, reduced trabeculation and failure of septation (Kim et al., 2001b), although single mutations of *Bmp6* or *Bmp7* did not induce any defects in the heart (Dudley et al., 1995; Luo et al., 1995; Solloway et al., 1998). As Bmp signaling inhibits myogenic differentiation synergistically with Notch1 signaling in C2C12 cells (Dahlqvist et al., 2003), this synergistic effect might lead to the suppression of myocardial differentiation in NICD1-activated ventricles.

Although NICD1 is activated in both sides (left and right) of the atrium and ventricle in the NICD1-activated heart, the strong induction of *Wnt2* and *Bmp6* was restricted to the left ventricle, whereas *Tnni2* and *Jag1* are induced in both sides of the ventricle. The reason for the restriction of *Wnt2* and *Bmp6* is currently unknown, but it may suggest the different responsiveness between the left and right ventricles to NICD1. The upregulation of these genes in NICD1-activated hearts was not mediated by Hesr1 and therefore might be regulated by direct binding of Rbpsuh to the enhancer region or by other Hes genes. Multiple putative binding sites for Su (H) (Rbpsuh) (more than 80% homology to consensus sequence) and also Hairy-binding sites (N-box sites) are present within the 10 kb upstream and downstream flanking regions of the *Wnt2*, *Bmp6*, *Tnni2* and *Jag1* transcription start sites (TFSEARCH; http://mbs.cbrc.jp/research/db/TFSEARCH.html). However, further enhancer analyses will be required to determine their functional relevance.

Our present study was initially designed to further understand the function of Notch signaling during cell fate decisions by ectopically expressing activated Notch1 in their precursors. Although we did not observe any cell fate changes during cardiac development, our detailed analyses of transgenic mouse phenotypes and downstream target genes enabled us to uncover several important aspects of Notch signaling in cardiac development. The functional differences between Hesr1 and Hesr2 are now of great interest in these events, and understanding the crosstalk between Notch and other signaling pathways, such as Wnt or Bmp, are obviously crucial for correct heart development. Further studies using gain- or loss-of-function experiments will now be required to fully elucidate the molecular mechanisms underlying cardiac development in the mouse.

We are grateful to Dr Hiroaki Nagao for the electron microscopic analysis, to Dr Satoshi Kitajima for helpful advice and discussions about Microarray analysis, and to the *Mesp1*-lineage experiments and Dr Tasuku Honjo for generously providing the *Rbpsuh* mutant mice. We would also like to

acknowledge our colleagues who provided us with cDNAs for use as probes, including Drs R. A. Conlon (*Notch1*), T. A. Mitsiadis (*Jag1*), I. Satokata (*Anf*), M. Shirai (*Tbx2*), M. E. Dickinson (*Bmp2*) and T. Takeuchi (*Hand1*). We also thank Ms Yuki Takahashi and Ms Yuka Sato for technical assistance, and Mr Okamura and Mr Oginuma for their support. This work was supported by the Organized Research Combination System and National BioResource Project of the Ministry of Education, Culture, Sports, Science and Technology, Japan.

Supplementary material

Supplementary material for this article is available at
http://dev.biologists.org/cgi/content/full/133/9/1625/DC1

References

Artavanis-Tsakonas, S., Rand, M. D. and Lake, R. J. (1999). Notch signaling: cell fate control and signal integration in development. *Science* **284**, 770-776.
Buckingham, M., Meilhac, S. and Zaffran, S. (2005). Building the mammalian heart from two sources of myocardial cells. *Nat. Rev. Genet.* **6**, 826-835.
Clark, K. A., McElhinny, A. S., Beckerle, M. C. and Gregorio, C. C. (2002). Striated muscle cytoarchitecture: an intricate web of form and function. *Annu. Rev. Cell Dev. Biol.* **18**, 637-706.
Dahlqvist, C., Blokzijl, A., Chapman, G., Falk, A., Dannaeus, K., Ibanez, C. F. and Lendahl, U. (2003). Functional Notch signaling is required for BMP4-induced inhibition of myogenic differentiation. *Development* **130**, 6089-6099.
de la Cruz, M. and Miller, B. (1968). Double-inlet ventricle: two pathological speciments with comments on the embryology alid on its relation to single ventricle. *Circulation* **37**, 249-260.
Donovan, J., Kordylewska, A., Jan, Y. N. and Utset, M. F. (2002). Tetralogy of fallot and other congenital heart defects in Hey2 mutant mice. *Curr. Biol.* **12**, 1605-1610.
Dudley, A. T., Lyons, K. M. and Robertson, E. J. (1995). A requirement for bone morphogenetic protein-7 during development of the mammalian kidney and eye. *Genes Dev.* **9**, 2795-2807.
Fischer, A., Schumacher, N., Maier, M., Sendtner, M. and Gessler, M. (2004). The Notch target genes Hey1 and Hey2 are required for embryonic vascular development. *Genes Dev.* **18**, 901-911.
Garg, V., Muth, A. N., Ransom, J. F., Schluterman, M. K., Barnes, R., King, I. N., Grossfeld, P. D. and Srivastava, D. (2005). Mutations in NOTCH1 cause aortic valve disease. *Nature* **437**, 270-274.
Gessler, M., Knobeloch, K. P., Helisch, A., Amann, K., Schumacher, N., Rohde, E., Fischer, A. and Leimeister, C. (2002). Mouse gridlock: no aortic coarctation or deficiency, but fatal cardiac defects in *Hey2*$^{-/-}$ mice. *Curr. Biol.* **12**, 1601-1604.
Gordon, A. M., Homsher, E. and Regnier, M. (2000). Regulation of contraction in striated muscle. *Physiol. Rev.* **80**, 853-924.
Hamada, Y., Kadokawa, Y., Okabe, M., Ikawa, M., Coleman, J. R. and Tsujimoto, Y. (1999). Mutation in ankyrin repeats of the mouse Notch2 gene induces early embryonic lethality. *Development* **126**, 3415-3424.
Han, Z. and Bodmer, R. (2003). Myogenic cells fates are antagonized by Notch only in asymmetric lineages of the Drosophila heart, with or without cell division. *Development* **130**, 3039-3051.
Huang, X., Pi, Y., Lee, K. J., Henkel, A. S., Gregg, R. G., Powers, P. A. and Walker, J. W. (1999). Cardiac troponin I gene knockout: a mouse model of myocardial troponin I deficiency. *Circ. Res.* **84**, 1-8.
Iso, T., Sartorelli, V., Chung, G., Shichinohe, T., Kedes, L. and Hamamori, Y. (2001a). HERP, a new primary target of Notch regulated by ligand binding. *Mol. Cell. Biol.* **21**, 6071-6079.
Iso, T., Sartorelli, V., Poizat, C., Iezzi, S., Wu, H. Y., Chung, G., Kedes, L. and Hamamori, Y. (2001b). HERP, a novel heterodimer partner of HES/E(spl) in Notch signaling. *Mol. Cell. Biol.* **21**, 6080-6089.
Iso, T., Chung, G., Hamamori, Y. and Kedes, L. (2002). HERP1 is a cell type-specific primary target of Notch. *J. Biol. Chem.* **277**, 6598-6607.
Iso, T., Kedes, L. and Hamamori, Y. (2003). HES and HERP families: multiple effectors of the Notch signaling pathway. *J. Cell Physiol.* **194**, 237-255.
Kaneta, M., Osawa, M., Sudo, K., Nakauchi, H., Farr, A. G. and Takahama, Y. (2000). A role for pref-1 and HES-1 in thymocyte development. *J. Immunol.* **164**, 256-264.
Kim, J. S., Viragh, S., Moorman, A. F., Anderson, R. H. and Lamers, W. H. (2001a). Development of the myocardium of the atrioventricular canal and the vestibular spine in the human heart. *Circ. Res.* **88**, 395-402.
Kim, R. Y., Robertson, E. J. and Solloway, M. J. (2001b). Bmp6 and Bmp7 are required for cushion formation and septation in the developing mouse heart. *Dev. Biol.* **235**, 449-466.
Kitajima, S., Miyagawa-Tomita, S., Inoue, T., Kanno, J. and Saga, Y. (2006). Mesp1-nonexpressing cells contribute to the ventricular cardiac conduction system. *Dev. Dyn.* **235**, 395-402.
Kokubo, H., Miyagawa-Tomita, S., Tomimatsu, H., Nakashima, Y., Nakazawa, M., Saga, Y. and Johnson, R. L. (2004). Targeted disruption of hesr2 results in atrioventricular valve anomalies that lead to heart dysfunction. *Circ. Res.* **95**, 540-547.
Kokubo, H., Miyagawa-Tomita, S., Nakazawa, M., Saga, Y. and Johnson, R. L. (2005). Mouse hesr1 and hesr2 genes are redundantly required to mediate Notch signaling in the developing cardiovascular system. *Dev. Biol.* **278**, 301-309.
Leimeister, C., Externbrink, A., Klamt, B. and Gessler, M. (1999). Hey genes: a novel subfamily of hairy- and Enhancer of split related genes specifically expressed during mouse embryogenesis. *Mech. Dev.* **85**, 173-177.
Luo, G., Hofmann, C., Bronckers, A. L., Sohocki, M., Bradley, A. and Karsenty, G. (1995). BMP-7 is an inducer of nephrogenesis, and is also required for eye development and skeletal patterning. *Genes Dev.* **9**, 2808-2820.
Ma, L., Lu, M. F., Schwartz, R. J. and Martin, J. F. (2005). Bmp2 is essential for cardiac cushion epithelial-mesenchymal transition and myocardial patterning. *Development* **132**, 5601-5611.
McCright, B., Lozier, J. and Gridley, T. (2002). A mouse model of Alagille syndrome: Notch2 as a genetic modifier of Jag1 haploinsufficiency. *Development* **129**, 1075-1082.
Miyagawa-Tomita, S., Morishima, M., Nakazawa, M., Mizutani, M. and Kikuchi, T. (1996). Pathological study of Japanese quail embryo with acid alpha-glucosidase deficiency during early development. *Acta Neuropathol. (Berl)* **92**, 249-254.
Monkley, S. J., Delaney, S. J., Pennisi, D. J., Christiansen, J. H. and Wainwright, B. J. (1996). Targeted disruption of the Wnt2 gene results in placentation defects. *Development* **122**, 3343-3353.
Nakagawa, O., Nakagawa, M., Richardson, J. A., Olson, E. N. and Srivastava, D. (1999). HRT1, HRT2, and HRT3: a new subclass of bHLH transcription factors marking specific cardiac, somitic, and pharyngeal arch segments. *Dev. Biol.* **216**, 72-84.
Nakagawa, O., McFadden, D. G., Nakagawa, M., Yanagisawa, H., Hu, T., Srivastava, D. and Olson, E. N. (2000). Members of the HRT family of basic helix-loop-helix proteins act as transcriptional repressors downstream of Notch signaling. *Proc. Natl. Acad. Sci. USA* **97**, 13655-13660.
Neuhaus, H., Rosen, V. and Thies, R. S. (1999). Heart specific expression of mouse BMP-10 a novel member of the TGF-beta superfamily. *Mech. Dev.* **80**, 181-184.
Nongthomba, U., Clark, S., Cummins, M., Ansari, M., Stark, M. and Sparrow, J. C. (2004). Troponin I is required for myofibrillogenesis and sarcomere formation in Drosophila flight muscle. *J. Cell Sci.* **117**, 1795-1805.
Noseda, M., McLean, G., Niessen, K., Chang, L., Pollet, I., Montpetit, R., Shahidi, R., Dorovini-Zis, K., Li, L., Beckstead, B. et al. (2004). Notch activation results in phenotypic and functional changes consistent with endothelial-to-mesenchymal transformation. *Circ. Res.* **94**, 910-917.
Pandur, P., Lasche, M., Eisenberg, L. M. and Kuhl, M. (2002). Wnt-11 activation of a non-canonical Wnt signalling pathway is required for cardiogenesis. *Nature* **418**, 636-641.
Park, M., Yaich, L. E. and Bodmer, R. (1998). Mesodermal cell fate decisions in Drosophila are under the control of the lineage genes numb, Notch, and sanpodo. *Mech. Dev.* **75**, 117-126.
Reaume, A. G., Conlon, R. A., Zirngibl, R., Yamaguchi, T. P. and Rossant, J. (1992). Expression analysis of a Notch homologue in the mouse embryo. *Dev. Biol.* **154**, 377-387.
Rones, M. S., McLaughlin, K. A., Raffin, M. and Mercola, M. (2000). Serrate and Notch specify cell fates in the heart field by suppressing cardiomyogenesis. *Development* **127**, 3865-3876.
Saga, Y., Miyagawa-Tomita, S., Takagi, A., Kitajima, S., Miyazaki, J. and Inoue, T. (1999). MesP1 is expressed in the heart precursor cells and required for the formation of a single heart tube. *Development* **126**, 3437-3447.
Saga, Y., Kitajima, S. and Miyagawa-Tomita, S. (2000). Mesp1 expression is the earliest sign of cardiovascular development. *Trends Cardiovasc. Med.* **10**, 345-352.
Sakata, Y., Kamei, C. N., Nakagami, H., Bronson, R., Liao, J. K. and Chin, M. T. (2002). Ventricular septal defect and cardiomyopathy in mice lacking the transcription factor CHF1/Hey2. *Proc. Natl. Acad. Sci. USA* **99**, 16197-16202.
Schroeder, T., Fraser, S. T., Ogawa, M., Nishikawa, S., Oka, C., Bornkamm, G. W., Honjo, T. and Just, U. (2003). Recombination signal sequence-binding protein Jkappa alters mesodermal cell fate decisions by suppressing cardiomyogenesis. *Proc. Natl. Acad. Sci. USA* **100**, 4018-4023.
Shirayoshi, Y., Yuasa, Y., Suzuki, T., Sugaya, K., Kawase, E., Ikemura, T. and Nakatsuji, N. (1997). Proto-oncogene of int-3, a mouse Notch homologue, is expressed in endothelial cells during early embryogenesis. *Genes Cells* **2**, 213-224.
Solloway, M. J., Dudley, A. T., Bikoff, E. K., Lyons, K. M., Hogan, B. L. and Robertson, E. J. (1998). Mice lacking Bmp6 function. *Dev. Genet.* **22**, 321-339.
Takahashi, Y., Koizumi, K., Takagi, A., Kitajima, S., Inoue, T., Koseki, H. and Saga, Y. (2000). Mesp2 initiates somite segmentation through the Notch signalling pathway. *Nat. Genet.* **25**, 390-396.
Terami, H., Hidaka, K., Katsumata, T., Iio, A. and Morisaki, T. (2004). Wnt11 facilitates embryonic stem cell differentiation to Nkx2.5-positive cardiomyocytes. *Biochem. Biophys. Res. Commun.* **325**, 968-975.
Timmerman, L. A., Grego-Bessa, J., Raya, A., Bertran, E., Perez-Pomares, J. M., Diez, J., Aranda, S., Palomo, S., McCormick, F., Izpisua-Belmonte, J. C.

et al. (2004). Notch promotes epithelial-mesenchymal transition during cardiac development and oncogenic transformation. *Genes Dev.* **18**, 99-115.
Wenink, A. C. (1981). Embryology of the ventricular septum. Separate origin of its components. *Virchows Arch. A Pathol. Anat. Histol.* **390**, 71-79.
Williams, R., Lendahl, U. and Lardelli, M. (1995). Complementary and combinatorial patterns of Notch gene family expression during early mouse development. *Mech. Dev.* **53**, 357-368.
Yamauchi, Y., Abe, K., Mantani, A., Hitoshi, Y., Suzuki, M., Osuzu, F., Kuratani, S. and Yamamura, K. (1999). A novel transgenic technique that allows specific marking of the neural crest cell lineage in mice. *Dev. Biol.* **212**, 191-203.
Zhu, L., Lyons, G. E., Juhasz, O., Joya, J. E., Hardeman, E. C. and Wade, R. (1995). Developmental regulation of troponin I isoform genes in striated muscles of transgenic mice. *Dev. Biol.* **169**, 487-503.

Available online at www.sciencedirect.com
SCIENCE DIRECT®
ELSEVIER
Reproductive Toxicology xxx (2005) xxx–xxx
Reproductive Toxicology
www.elsevier.com/locate/reprotox

Reproductive and developmental toxicity screening test of basic rubber accelerator, 1,3-di-*o*-tolylguanidine, in rats

Makoto Ema [a,*], Eisuke Kimura [b], Mariko Matsumoto [a], Akihiko Hirose [a], Eiichi Kamata [a]

[a] *Division of Risk Assessment, Biological Safety Research Center, National Institute of Health Sciences, Tokyo, Japan*
[b] *Panapharm Laboratories Co., Ltd., Uto, Japan*

Received 8 July 2005; received in revised form 1 November 2005; accepted 7 November 2005

Abstract

Twelve male and female rats per group were exposed to the rubber accelerator 1,3-di-*o*-tolylguanidine (DTG) by gavage at 0, 8, 20 or 50 mg/kg bw/day. Males were dosed for a total of 49 days beginning 14 days before mating. Females were dosed for a total of 40–49 days beginning 14 days before mating to day 3 of lactation throughout the mating and gestation period. At 50 mg/kg bw/day, deaths were observed in two males and three females. Lowered body weight gain and food consumption were noted in males at 50 mg/kg bw/day and females at 20 and 50 mg/kg bw/day. Mydriasis, decreased locomotor activity, bradypnea, prone position, tremor and/or salivation were observed in males and females at 20 and 50 mg/kg bw/day. No effects of DTG were found on the estrous cyclicity, precoital interval, copulation, fertility and gestational indices, numbers of corpora lutea and implantations, or gestation length. A significant decrease in the number, body weight and viability of offspring and increase in the incidence of fetuses with external malformations were found at 50 mg/kg bw/day. Oligodactyly, anal atresia and tail anomalies were observed. These data suggest that DTG may be teratogenic. The NOAELs of DTG for general and developmental toxicity in rats are 8 and 20 mg/kg bw/day, respectively.

Keywords: Di-*o*-tolylguanidine; Rubber accelerator; Sigma ligand; Reproductive and developmental toxicity; Teratogenicity; Malformation; Rat

1. Introduction

The basic rubber accelerator 1,3-di-*o*-tolylguanidine (CAS No. 97-39-2; DTG) is produced in the million pound range annually in the United States [1,2]. DTG is known as a selective sigma ligand [3]. In this context, many pharmacological studies of DTG were performed [3–12]. Ligands that interact with sigma sites have been shown to produce hypothermia [4–6]. Hypothermia induced by DTG was detected following subcutaneous or intracerebroventricle injection in rats [5,6] and intraperitoneal injection in mice [4]. The intraperitoneal injection of DTG potently reduced the pain behavior in the acute but increased pain behavior in the tonic phase in the formalin test in mice [7]. Intraperitoneal injection of DTG produced significant but short-lived increases in the withdrawal latencies in mice [4]. Bastianetto et al. [8] showed that unilateral intranigral injection caused circulating behavior in rats and suggested that sigma sites play a role in movement and posture through their association with brainstem and forebrain motor control circuits. Decreased locomotor activity induced by intraperitoneal injection [9,10], increased bladder capacity induced by intravenous injection in the anaesthetized condition [11] and no change in immobility time in open field after intraperitoneal injection [12] were also reported in rats given DTG. Toxicological studies on DTG have given little information on acute animal toxicity [13]: intraperitoneal LD50 was 25 mg/kg bw in mice; oral LD50 was 500 mg/kg bw in rats; lowest published lethal dose of oral administration was 80 mg/kg bw in rabbits; and the lowest published lethal dose was 120 mg/kg bw after oral administration in mammals, species unspecified. At the present time, no information is available for the reproductive and developmental toxicity of DTG. It is generally assumed that the results of animal test on chemical toxicity are relevant to human health [14]. As such, the testing for reproductive and developmental toxicity

* Corresponding author. Tel.: +81 3 3700 9878; fax: +81 3 3707 1408.
E-mail address: ema@nihs.go.jp (M. Ema).

0890-6238/$ – see front matter © 2005 Elsevier Inc. All rights reserved.
doi:10.1016/j.reprotox.2005.11.002

in animal models is an important part of the overall toxicology. The present study was conducted to obtain information on the effects of DTG on reproductive and developmental parameters in rats.

2. Materials and methods

This study was performed in compliance with OECD guideline 421 Reproduction/Developmental Toxicity Screening Test [15] and in accordance with the principles for Good Laboratory Practice [16,17] and "Guidance for Animal Care and Use" of Panapharm Laboratories Co., Ltd.

2.1. Animals

International Genetic Standard (Crj: CD (SD) IGS) rats were used throughout this study. This strain was chosen because it is most commonly used in toxic studies, including reproductive and developmental toxicity studies, and historical control data are available. Males and females at 8 weeks of age were purchased from Atsugi Breeding Center, Charles River Japan, Inc. (Yokohama, Japan). The rats were acclimated to the laboratory for 13 days prior to the start of the experiment. Male and female rats found to be in good health were selected for use. Vaginal smears of each female were recorded and only females showing a 4-day estrous cycle were used in the experiment. Male and female rats were distributed on a random basis into four groups of 12 males and 12 females each. Rats were housed individually, except during the acclimation, mating and nursing periods. From day 0 of pregnancy to the day of sacrifice, individual dams and litters were reared using wooden chips as bedding (White Flake; Charles River Japan, Inc.).

Animals were reared on a sterilized basal diet (CRF-1; Oriental Yeast Co., Ltd., Tokyo, Japan) and sterilized water ad libitum and maintained in an air-conditioned room at 24 ± 2 °C, with a relative humidity of 55 ± 10%, a 12-h light/12-h dark cycle and ventilation with 13–15 air charges per hour.

2.2. Chemicals and dosing

DTG was obtained from Sumitomo Chemical Co., Ltd. (Tokyo, Japan). DTG, a white powder, is slightly soluble in hot water and alcohol, soluble in chloroform and very soluble in ether, and its melting point is 179 °C, specific gravity is 1.10 and molecular weight is 239.3 [2]. The DTG (Lot No. 30J08) used in this study was 99.6% pure, and it was kept in a dark place at room temperature. The purity and stability of the chemical were verified by analysis before the study. Rats were dosed once daily by gastric intubation with DTG at a dose of 0 (control), 8, 20 or 50 mg/kg bw. The dosage levels were determined based on the results of our previous dose-finding study, the 14-day repeated dose toxicity study in rats given DTG by gavage at 0, 10, 20, 40 or 80 mg/kg bw/day, in which deaths were found at 80 mg/kg bw/day, decreased locomotor activity, mydriasis, tremor and salivation were observed at 40 and 80 mg/kg bw/day, and no adverse effects were detected at 10 and 20 mg/kg bw/day (data not shown). DTG was suspended in 0.5% (w/v) carboxymethylcellulose-Na solution with 0.1% (w/v) Tween 80. Males (12 rats/group) were dosed for a total of 49 days beginning 14 days before mating. Females (12 rats/group) were dosed for a total of 40–49 days beginning 14 days before mating to day 3 of lactation throughout the mating and gestation period. The volume of each dose was adjusted to 10 ml/kg body weight based on the latest body weight during the re-mating and mating period in males and females or the body weight on day 0 of pregnancy in females after copulation. Control rats were given 0.5% (w/v) carboxymethylcellulose-Na solution with 0.1% (w/v) Tween 80. The stability of formulations has been confirmed for up to 8 days. During use, the formulations were maintained under such conditions for less than 7 days, and the target concentration was 96.5 to 101.4%.

2.3. Observations

All rats were observed daily for clinical signs of toxicity. The body weight was recorded twice a week in males, and twice a week during the pre-mating and mating periods, on days 0, 7, 14 and 21 of pregnancy and on days 0 and 4 of lactation in females. Food consumption was recorded twice weekly during the pre-mating period in males, and twice weekly during the pre-mating period, on days 1, 7, 14 and 21 of pregnancy and on days 1 and 4 of lactation in females. The rats were euthanized by exsanguination under anesthesia on the next day of the last administration in males and on day 4 of lactation in females. The external surfaces of the rats were examined. The abdomen and thoracic cavity were opened, and gross internal examination was performed. In males, the testes and epididymides were weighed. In females, the numbers of corpora lutea and implantation sites and weight of the ovaries were recorded. The testes and epididymides were fixed with Bouin's solution and preserved in 10% neutral buffered formalin, and the ovaries were stored in 10% neutral buffered formalin. Histopathological evaluations were performed on hematoxylin–eosin-stained tissue sections of these organs.

Daily vaginal lavage samples of each female were evaluated for estrous cyclicity throughout the pre-mating period. Each female rat was mated overnight with a single male rat of the same dosage group until copulation occurred or the mating period, 2 weeks, had elapsed. During the mating period, daily vaginal smears were examined for the presence of sperm. The presence of the sperm in the vaginal smear and/or a vaginal plug was considered evidence for successful mating. Once insemination was confirmed, the females were checked for signs of parturition before noon from day 20 of pregnancy. The females were allowed to deliver spontaneously and nurse their pups until postnatal day (PND) 4. The day on which parturition was completed by 12:00 was designated as PND 0. Litter size and numbers of live and dead pups were recorded. Gender was determined on live pups examined grossly and individually weighed on PNDs 0 and 4. On PND 4, the pups were euthanized by exsanguination under anesthesia and gross internal examinations were performed.

2.4. Data analysis

The statistical analysis of pups was carried out using the litter as the experimental unit. The body weight, body weight gain, food consumption, length of estrous cycles, precoital interval, gestation length, weight of the organs, relative organ weight, numbers of corpora lutea, implantations and live and dead pups, total number of pups and weight of live pups were analyzed with Bartlett's test for homogeneity of variance at the 5% level of significance. If homogeneous the data were analyzed using Dunnett's multiple comparison test to compare the mean of the control group with that of each dosage group. If not, the DTG-treated groups were compared with that of the control group with Steel's multiple comparison test. The implantation, delivery and viability indexes, and incidence of pups with anomalies and individual anomalies were analyzed with Wilcoxon's rank sum test. The mortality, copulation, fertility and gestation indexes, and sex ratio of pups were analyzed with Fisher's exact test. The 5% level of probability was used as the criterion for significant.

3. Results

Table 1 shows the findings in male rats given DTG. At 50 mg/kg bw/day, one male died after six administrations and one male died after seven administrations. These dead rats showed mydriasis, decreased locomotor activity, bradypnea, a prone position and tremor 10–20 min after the administration of DTG. In surviving males, mydriasis, decreased locomotor activity, bradypnea and prone position on days 1–9 of the administration period, tremor during the whole period of administration and salivation on days 22–49 of the administration period were also observed at 50 mg/kg bw/day. Salivation was noted on days 28–49 of the administration period at 20 mg/kg bw/day. A significant decrease in the body weight gain was found on days 1–8 (81% decrease) and days 15–22 (48% decrease) of the administration period at 50 mg/kg bw/day. At this dose, significantly lower food consumption on days 7–8 (20% decrease) and days 14–15 (7% decrease) of the administration period was also observed.

Table 1
Findings in male rats given DTG

	Dose (mg/kg bw/day)			
	0 (control)	8	20	50
No. of male rats	12	12	12	12
No. of deaths during pre-mating period	0	0	0	2
Initial body weight (g)[a]	381 ± 16	379 ± 16	378 ± 15	380 ± 16
Body weight gain (g)[a]				
Days 1–8	30 ± 7	33 ± 7	25 ± 7	6 ± 9**
Days 8–15	29 ± 5	32 ± 5	32 ± 7	24 ± 7
Days 15–22	23 ± 6	25 ± 8	23 ± 7	12 ± 11**
Days 22–29	19 ± 9	22 ± 7	25 ± 8	19 ± 5
Days 29–36	22 ± 6	22 ± 6	23 ± 7	18 ± 8
Days 36–43	15 ± 8	12 ± 9	13 ± 5	14 ± 7
Days 43–50	19 ± 8	19 ± 7	13 ± 4	13 ± 11
Food consumption (g/day/rat)[a]				
Days 7–8	25 ± 3	26 ± 3	26 ± 2	20 ± 3**
Days 14–15	29 ± 2	30 ± 2	29 ± 3	27 ± 3*
Days 29–30	27 ± 2	27 ± 3	28 ± 3	25 ± 2
Days 35–36	28 ± 2	29 ± 2	29 ± 2	27 ± 2
Days 42–43	26 ± 3	25 ± 3	27 ± 4	27 ± 3
Days 49–50	28 ± 4	29 ± 3	28 ± 2	28 ± 3

[a] Values are given as the mean ± S.D.
* Significantly different from the control group ($p < 0.05$).
** Significantly different from the control group ($p < 0.01$).

Table 2 presents the findings in female rats given DTG. At 50 mg/kg bw/day, two females died after the first administration and one female died after normal delivery of her pups on day 22 of pregnancy. Mydriasis, decreased locomotor activity, bradypnea, prone position, and tremor and salivation 10–20 min after the administration of DTG were observed in females died after the first administration. These clinical signs and salivation were found during pregnancy and on day of parturition in a female which died after parturition. In surviving females, mydriasis, decreased locomotor activity, bradypnea and prone position on day 1 of the administration period to day 0 of lactation, tremor on day 1 of the administration period to day 5 of pregnancy and salivation on day 4 of pregnancy to day 3 of lactation were observed at 50 mg/kg bw/day. Mydriasis, decreased locomotor

Table 2
Findings in female rats given DTG

	Dose (mg/kg bw/day)			
	0 (control)	8	20	50
No. of female rats	12	12	12	12
No. of deaths during pre-mating period	0	0	0	2
No. of deaths during pregnancy	0	0	0	1
Initial body weight (g)[a]	381 ± 16	379 ± 16	378 ± 15	380 ± 16
Body weight gain (g)[a]				
Days 1–8	19 ± 8	17 ± 7	11 ± 6*	−1 ± 9**
Days 8–15	10 ± 7	15 ± 8	20 ± 5**	15 ± 10
Days 0–7 of pregnancy	34 ± 6	31 ± 6	33 ± 4	28 ± 8
Days 7–14 of pregnancy	34 ± 5	34 ± 4	36 ± 3	30 ± 10
Days 14–21 of pregnancy	85 ± 17	100 ± 14	105 ± 9*	42 ± 21**
Days 0–4 of lactation	20 ± 19	14 ± 16	22 ± 9	16 ± 13
Food consumption (g/day/rat)[a]				
Days 7–8	22 ± 3	21 ± 2	19 ± 2**	13 ± 3**
Days 14–15	20 ± 4	22 ± 3	22 ± 2	20 ± 2
Days 6–7 of pregnancy	22 ± 3	23 ± 2	23 ± 3	17 ± 3**
Days 13–14 of pregnancy	23 ± 2	24 ± 3	25 ± 2	22 ± 5
Days 20–21 of pregnancy	24 ± 4	26 ± 3	29 ± 3*	21 ± 5
Days 3–4 of lactation	41 ± 5	41 ± 3	46 ± 4*	32 ± 6**

[a] Values are given as the mean ± S.D.
* Significantly different from the control group ($p < 0.05$).
** Significantly different from the control group ($p < 0.01$).

Table 3
Reproductive findings in rats given DTG

	Dose (mg/kg bw/day)			
	0 (control)	8	20	50
No. of pairs	12	12	12	10
Length of estrous cycles (day)[a]	4.0 ± 0.2	4.1 ± 0.3	4.1 ± 0.3	4.1 ± 0.2
Precoital interval (day)[a]	3.0 ± 1.0	2.7 ± 1.0	2.4 ± 1.1	2.2 ± 1.0
Copulation index (%)[b]				
Male	100	91.7	100	100
Female	100	91.7	100	100
Fertility index (%)[c]	100	100	91.7	100
Gestation index (%)[d]	100	100	100	90.0
Gestation length (day)[a]	22.6 ± 0.5	22.3 ± 0.5	22.5 ± 0.5	22.6 ± 0.5
Weight of testes (g)[a]	3.24 ± 0.34	3.34 ± 0.19	3.31 ± 0.28	3.30 ± 0.24
Relative weight of testes[a,e]	0.60 ± 0.05	0.62 ± 0.07	0.63 ± 0.07	0.68 ± 0.07*
Weight of epididymides (g)[a]	1.16 ± 0.10	1.21 ± 0.06	1.21 ± 0.12	1.23 ± 0.07
Relative weight of epididymides[a,e]	0.22 ± 0.02	0.22 ± 0.02	0.23 ± 0.03	0.25 ± 0.02**
Weight of ovaries (mg)[a]	101 ± 8	106 ± 6	101 ± 11	102 ± 10
Relative weight of ovaries[a,e]	30 ± 2	31 ± 2	28 ± 3	32 ± 2

[a] Values are given as the mean ± S.D.
[b] Copulation index (%) = (no. of rats copulated/no. of pairs) × 100.
[c] Fertility index (%) = (no. of females pregnant/no. of females copulated) × 100.
[d] Gestation index (%) = (no. of females with parturition/no. of females copulated) × 100.
[e] Relative weight = organ weight/100 g of body weight.
* Significantly different from the control group ($p < 0.05$).
** Significantly different from the control group ($p < 0.01$).

activity, bradypnea and prone position on days 2–3 of the administration period, and salivation on day 14 of pregnancy to day 3 of lactation were observed at 20 mg/kg bw/day. Body weight gain was significantly lowered on days 1–8 of the pre-mating period at 20 mg/kg bw/day (42% decrease) and on days 1–8 of the pre-mating period (105% decrease) and days 14–21 of pregnancy (49% decrease) at 50 mg/kg bw/day. At 20 mg/kg bw/day, a significantly higher body weight gain was observed on days 8–15 of the pre-mating period and days 14–21 of pregnancy. Food consumption was significantly reduced on days 7–8 of the pre-mating period at 20 mg/kg bw/day (14% decrease) and on days 7–8 of the pre-mating period (41% decrease) and days 3–4 of lactation (24% decrease) at 50 mg/kg bw/day. At 20 mg/kg bw/day, a significant increase in the food consumption was observed on days 20–21 of pregnancy and days 3–4 of lactation.

The reproductive findings in rats given DTG are presented in Table 3. No effects of DTG were observed on the length of estrous cycles, precoital interval and gestation length. One pair did not copulate at 8 mg/kg bw/day, one female did not become impregnated at 20 mg/kg bw/day and one female did not deliver any pups at 50 mg/kg bw/day; however, no significant differences were noted in the copulation, fertility or gestation index between the control and DTG-treated groups. The weights of the testes and epididymides, and absolute weight and relative weight of the ovaries in the DTG-treated groups did not differ from the control group. The relative weights of the testes (13% increase) and epididymides (14% increase) were significantly higher at 50 mg/kg bw/day.

The developmental findings in rats given DTG are shown in Table 4. There was no significant difference in the numbers of corpora lutea, implantations and stillborns, implantation index, sex ratio of live pups, viability index on day 0 of lactation and body weight of live pups on day 4 of lactation between the control and DTG-treated groups. The numbers of pups delivered (45% decrease) and live pups delivered (45% decrease) and delivery index (43% decrease) were significantly lowered at 50 mg/kg bw/day. At this dose, the viability index on day 4 of lactation (34% decrease) and body weight of live male (16% decrease) and female (19% decrease) pups on day 0 of lactation were also significantly decreased. Two dams with totally litter loss were observed. No poor maternal behavior or nursing was observed in dams at 50 mg/kg bw/day. No histopathological changes were found in the testes, epididymides and ovaries in the DTG-treated groups. External anomalies in pups of rats given DTG are also presented in Table 4. No fetuses with external malformations were observed in the control and groups given DTG at 8 and 20 mg/kg bw/day. At 50 mg/kg bw/day, fetuses with external malformations were found in 10 out of the 65 fetuses and in 3 out of the 9 litters. Oligodactyly was observed in four pups in two litters. A kinked tail was found in six pups in one litter and a short tail and anal atresia was observed in one pup in each letter. Although there was no significant difference in the incidence of fetuses with individual malformations between the control and 50 mg/kg bw/day groups, a significantly higher incidence of total number of fetuses with external malformations was noted at this dose.

Table 4
Developmental findings in rats given DTG

	Dose (mg/kg bw/day)			
	0 (control)	8	20	50
No. of litters	12	11	11	9
No. of implantations[a]	14.3 ± 2.6	16.2 ± 1.9	15.9 ± 1.4	14.2 ± 3.6
Implantation index (%)[b]	92.2	94.7	97.6	90.9
No. of pups delivered[a]	13.0 ± 2.4	15.2 ± 2.0	14.7 ± 1.4	7.2 ± 4.1**
No. of live pups delivered[a]	13.0 ± 2.4	15.1 ± 1.9	14.7 ± 1.4	7.2 ± 4.1**
No. of stillborns	0	0.1 ± 0.3	0	0
Delivery index (%)[c]	91.0	93.3	92.2	51.7**
Sex ratio of live pups (males/females)	71/85	84/82	80/82	31/34
Viability index (%)[d,e]				
Day 0 of lactation	100	99.5	100	100
Day 4 of lactation	99.4	99.4	100	65.4**
Body weight of male pups during lactation (g)[a]				
Day 0	7.4 ± 0.7	6.9 ± 0.6	7.3 ± 0.6	6.2 ± 1.0**
Day 4	11.9 ± 1.3	11.1 ± 1.0	11.7 ± 1.0	11.0 ± 2.3
Body weight of female pups during lactation (g)[a]				
Day 0	7.0 ± 0.7	6.6 ± 0.6	6.8 ± 0.7	5.7 ± 0.8**
Day 4	11.4 ± 1.3	10.5 ± 1.0	11.0 ± 0.9	10.5 ± 2.0
External examination of pups				
No. of pups (litters) with malformations	0	0	0	10 (3)*
Oligodactyly	0	0	0	4 (2)
Kinky tail	0	0	0	6 (1)
Short tail	0	0	0	1
Anal atresia	0	0	0	1

[a] Values are given as the mean ± S.D.
[b] Implantation index (%) = (no. of implantations/no. of corpora lutea) × 100.
[c] Delivery index (%) = (no. of live pups delivered/no. of implantations) × 100.
[d] Viability index on day 0 of lactation (%) = (no. of live pups delivered/total no. of pups delivered) × 100.
[e] Viability index on day 4 of lactation (%) = (no. of live pups on day 4 of lactation/no. of live pups delivered) × 100.
* Significantly different from the control group ($p < 0.05$).
** Significantly different from the control group ($p < 0.01$).

4. Discussion

The present study was conducted to obtain initial information on the possible effects of DTG on reproduction and development in rats. The data show that DTG exerts developmental toxicity and suggest that DTG possesses teratogenic potential.

DTG was given to males during the pre-mating and mating periods and to females during the pre-mating, mating, pregnancy and shortly after parturition. The dosage used in the present study was sufficiently high such that it should be expected to induce general toxic and neurobehavioral effects. As expected, general toxicity, such as decreases in body weight gain and food consumption, was found at 50 mg/kg bw/day in males and at 20 and 50 mg/kg bw/day in females. Decreases in the body weight gain and food consumption during the early administration period, and thereafter, significant increases in body weight gain and food consumption were observed in females at 20 mg/kg bw/day. One possible explanation for increased body weight gain during late pregnancy at 20 mg/kg bw/day may be higher number of pups and higher net weight gain during pregnancy at this dose compared with the controls. Such recovery did not occur at the highest dose. Neurobehavioral effects, such as mydriasis, decreased locomotor activity, bradypnea, prone position, tremor and salivation, were also observed at 20 and 50 mg/kg bw/day. DTG is a specific sigma receptor ligand [3] and sigma receptor ligands can modulate neurotransmissions, including the noradrenergic, glutamatergic and dopaminergic system [10,18,19]. It was reported that systemic injection of DTG caused neurobehavioral changes in rats [5,6,9,10]. The present study shows that the oral administration of DTG also induces neurobehavioral changes, and it is neurobehaviorally toxic at 20 and 50 mg/kg bw/day in rats.

Higher relative weights, but not the absolute weight, of the testes and epididymides were observed at 50 mg/kg bw/day. Body weights of male rats on the day of scheduled sacrifice were 537 and 485 g in the control and 50 mg/kg bw/day groups, respectively. It seems likely that the higher relative weights of the testes and epididymides at the highest dose were due to secondarily lowered body weight but not due to the direct effects of DTG on the male reproductive organs. Other male reproductive parameters were not significantly changed, even at the highest dose. These findings suggest that DTG is not reproductively toxic to male rats. It seems unlikely that DTG exerts reproductive toxicity to female rats when administered during the pre-mating, mating, pregnancy and early lactation period, because no adverse effects on the maternal reproductive parameters, including estrous cyclicity, precoital interval, copulation

index, fertility index, gestation index, gestation length and ovarian weight, were caused by the administration of DTG in females.

As for the developmental indexes, decreases in the numbers of total pups and live pups delivered, delivery index, viability on PND 4 and body weight of live pups on PND 0 were detected at 50 mg/kg bw/day. These findings indicate that DTG is toxic to the survival and growth of offspring and exerts developmental toxicity at 50 mg/kg bw/day in rats.

In the present study, the teratogenic effect of DTG is strongly suggested by the external examinations of pups. At 50 mg/kg bw/day, a significant increase in the total number of fetuses with external malformations was noted; however, incidences of fetuses with individual types of external malformations at this dose were not significantly different from those in the control group. The external malformations observed in the present study are of the types that occur spontaneously among control rat fetuses reported in the literature [20–23]. In the present study, only external examination in the newborn rats was performed, and no internal or skeletal examinations were performed. Even animals not ordinarily carnivorous, including nonhuman primates, are likely to eat dead and moribund offspring, as well as those with malformations that involve skin lesions allowing the loss of body fluids or the exposure of viscera [24]. To accurately evaluate the prenatal developmental toxicity including teratogenicity, it is necessary to interrupt pregnancy 12–24 h before the expected term either by hysterectomy or the necropsy of maternal animals [24,25]. The present study was performed in compliance with OECD guideline 421 Reproduction/Developmental Toxicity Screening Test [15], and this screening test guideline does not provide complete information on all aspects of reproduction and development due to the relatively small numbers of animals in the dose groups and selectivity of the endpoints. In order to further evaluate the developmental toxicity, including teratogenicity, of DTG in rats, a prenatal developmental toxicity study is currently in progress.

In conclusion, DTG caused decreased body weight gain and food consumption at 50 mg/kg bw/day in males and at 20 and 50 mg/kg bw/day in females, neurobehavioral changes at 20 and 50 mg/kg bw/day in both sexes, and changes in developmental parameters at 50 mg/kg bw/day. DTG is suggested to be teratogenic. The NOAELs of DTG for general and developmental toxicity were 8 and 20 mg/kg bw/day, respectively, in rats.

Acknowledgements

This study was performed in 2002 at the Panapharm Laboratories Co., Ltd. (Uto, Japan) and supported by the Ministry of Health, Labour and Welfare, Japan.

References

[1] Scorecard. Chemical profile for 1,3-bis(*o*-tolyl)guanidine (CAS number: 97-39-2); 2005 [http://www.scorecard.org/chemical-profiles/summary.tcl?edf_substance_id=+97-39-2].
[2] TOXNET. *N,N'*-Bis(2-methylphenyl)guanidine; 2005 [http://toxnet.nlm.nih.gov/cgi-bin/sis/search/f?/temp].
[3] Weber E, Sonders M, Quarum M, Mclean S, Pou S, Keana JFW. 1,3-Di (2-(5-^{3}H)tolyl)guanidine: a selective ligand that labels σ-type receptors for psychotomimetic opiates and antipsychotic drugs. Proc Natl Acad Sci 1986;83:8784–8.
[4] Kest B, Mogil JS, Sternberg WF, Pechnick RN, Liebeskind JC. Antinociception following 1,3-di-*o*-tolylguanidine, a selective σ receptor ligand. Pharmacol Biochem Behav 1995;50:587–92.
[5] Bejanian M, Pechnick RN, Bova MP, George R. Effects of subcutaneous and intracerebroventricular administration of the *sigma* receptor ligand 1,3-di-*o*-tolylguanidine on body temperature in the rat: interactions with BMY 14802 and rimcazole. J Pharmacol Exp Ther 1991;258:88–93.
[6] Rawls SM, Baron DA, Geller EB, Adler MW. Sigma sites mediate DTG-evoked hypothermia in rats. Pharmacol Biochem Behav 2002;73:779–86.
[7] Kest B, Mogil JS, Sternberg WF, Pechnick RN, Liebeskind JC. 1,3-Di-*o*-tolylguanidine (DTG) differentially affects acute and tonic formalin pain: antagonism by rimcazole. Pharmacol Biochem Behav 1995;52:175–8.
[8] Bastianetto S, Perralt G, Sanger DJ. Pharmacological evidence for the involvement of sigma sites in DTG-induced contralateral circling in rats. Neuropharmacology 1995;34:107–14.
[9] Maj J, Rogóż Z, Skuza G. Some behavioral effects of 1,3-di-*o*-tolylguanidine, opipramol and seritraline, the sigma site ligands. Pol J Pharmacol 1996;48:379–95.
[10] Skuza G, Rogóż Z. Effects of 1,3-di-*o*-tolylguanidine (DTG), rimcazole and EMD 57445, the σ receptor ligands, in the forced swimming test. Pol J Pharmacol 1997;49:329–35.
[11] Shimizu I, Kawashima K, Ishii D, Oka M. Effects of (+)-pentazocine and 1,3-di-*o*-tolylguanidine (DTG), sigma (σ) ligands, on micturition in anaesthetized rats. Brit J Pharmacol 2000;131:610–6.
[12] Skuza G, Rogóż Z. Sigma receptor antagonists attenuate antidepressant-like effect induced by co-administration of 1,3di-*o*-tolylguanidine (DTG) and memantine in the forced swimming test in rats. Pol J Pharmacol 2003;55:1149–52.
[13] RTECS (The Registry of Toxic Effects of Chemical Substances). Guanidine, 1,3-di-*o*-tolyl; 2005 [http://www.cdc.gov/niosh/rtecs/mf155cc0.html].
[14] Clayson DB, Krewski DR. Objectives of toxicity testing. In: Arnold DL, Grice HC, Krewski DR, editors. Handbook of in vivo toxicity testing. San Diego: Academic Press; 1990. p. 3–18.
[15] OECD (Organization for Economic Co-operation and Development). OECD Test Guideline for Testing of Chemicals, No. 421, Reproduction/Developmental Toxicity Screening Test. Adopted by the Council on 27th July 1995. Paris; 1995.
[16] OECD (Organization for Economic Co-operation and Development). OECD Principles on Good Laboratory Practice (as revised in 1997). OECD Series on Principles of Good Laboratory Practice and Compliance Monitoring, No. 1. Paris; 1998.
[17] EA, MHW and MITI (Environment Agency, Ministry of Health and Welfare, and Ministry of International Trade and Industry of Japan). Research of Designated Chemical Substances, Planning and Coordination Bureau, Environment Agency, No. 39, Environmental Health Bureau, Ministry of Health and Welfare, No. 229, Basic Industries Bureau, Ministry of International Trade and Industry, No. 85, March 31, 1984, and amendments, November 18, 1988. Tokyo; 1988.
[18] Goldstein SR, Matsumoto RR, Thompson TL, Patrick RL, Bowen WD, Walker JM. Motor effects of two sigma ligands mediated by nigrostriatal dopamine neurons. Synapse 1989;4:254–8.
[19] Bastianetto S, Rouquier L, Perralt G, Sanger DJ. DTG-induced circling behaviour in rats may involve the interaction between σ sites and nigrostriatal dopaminergic pathways. Neuropharmacology 1995;34:281–7.
[20] Kameyama Y, Tanimura T, Yasuda M, editors. Spontaneous malformations in laboratory animals—photographic atlas and reference data. Cong Anom 1980;20:25–106.
[21] Morita H, Ariyuki F, Inomata N, Nishimura K, Hasegawa Y, Miyamoto M, et al. Spontaneous malformations in laboratory animals: frequency of external, internal and skeletal malformations in rats, rabbits and mice. Cong Anom 1987;27:147–206.
[22] Nakatsuka T, Horimoto M, Ito M, Matsubara Y, Akaike M, Ariyuki F. Japan Pharmaceutical Manufacturers Association (JPMA) survey on